Review

Skin Imaging Using Optical Coherence Tomography and Photoacoustic Imaging: A Mini-Review

Mohsin Zafar [ID], Amanda P. Siegel [ID], Kamran Avanaki [ID] and Rayyan Manwar *[ID]

Richard and Loan Hill Department of Biomedical Engineering, University of Illinois at Chicago, Chicago, IL 60607, USA; mzafar9@uic.edu (M.Z.); apsiegel@uic.edu (A.P.S.); avanaki@uic.edu (K.A.)
* Correspondence: rmanwar@uic.edu

Abstract: This article provides an overview of the progress made in skin imaging using two emerging imaging modalities, optical coherence tomography (OCT) and photoacoustic imaging (PAI). Over recent years, these technologies have significantly advanced our understanding of skin structure and function, offering non-invasive and high-resolution insights previously unattainable. The review begins by briefly describing the fundamental principles of how OCT and PAI capture images. It then explores the evolving applications of OCT in dermatology, ranging from diagnosing skin disorders to monitoring treatment responses. This article continues by briefly describing the capabilities of PAI imaging, and how PAI has been used for melanoma and non-melanoma skin cancer detection and characterization, vascular imaging, and more. The third section describes the development of multimodal skin imaging systems that include OCT, PAI, or both modes. A comparative analysis between OCT and PAI is presented, elucidating their respective strengths, limitations, and synergies in the context of skin imaging.

Keywords: optical coherence tomography; OCT; skin; photoacoustic imaging; PAI

1. Introduction

In the dynamic realm of medical diagnostics and healthcare, technological advancements are enhancing our understanding of physiological processes and enabling improved patient care in many ways including faster, less invasive diagnoses, improved treatment monitoring, and more [1]. Among the many areas witnessing such progress, skin imaging stands out, as these emerging technologies have profound implications for dermatology, plastic surgery, and overall healthcare management. This review describes two cutting-edge imaging modalities—optical coherence tomography (OCT) and photoacoustic imaging (PAI)—that are revolutionizing clinical care by offering unprecedented insights into skin structure and function that can lead to significant reductions in skin biopsies, leading to reduced morbidity which otherwise often relies on skin biopsies [2,3]. The reduction in or elimination of the need for skin biopsies for diagnosis and treatment monitoring not only decreases discomfort, reduces scarring, speeds up recovery, and minimizes risk from complications, but it also often enables non-invasive treatment monitoring that is otherwise not available. Treatment monitoring at the cellular level is an important element of personalized medicine, permitting the assessment of an individual's response to a specific treatment plan and individualized therapy, which can also improve outcomes. This is particularly important for monitoring interactions between the immune system and inflammatory and autoimmune skin pathologies [4].

The skin, the largest organ of the human body, serves as a protective barrier against external threats while harboring complex structures that reflect overall health [1]. Traditional imaging techniques, though valuable, often provide limited depth and/or resolution, constraining our ability to explore the intricate layers of the skin in order to identify and monitor the treatment of skin pathologies without the need for skin biopsy [5–9]. OCT and

PAI, two innovative technologies that have overcome these limitations, offer a non-invasive, high-resolution visualization of skin architecture and function [10]. OCT represents a milestone in medical imaging. In OCT, a broad-bandwidth light source is broken into two arms, the sample arm and a reference arm, and their interference patterns are analyzed. The use of low-coherence, broadband light produces a composite waveform of interference patterns that can be analyzed by Fourier transform, with the results combined to generate axial scans or A-lines. Commercial swept-source OCT can acquire 400,000 A-lines per second with an axial resolution from 2 to 10 μm and a lateral resolution from 1 to 10 μm, depending on the central frequency and other factors [11–14]. Clinically, the use of OCT for rapid and accurate assessment of the posterior segment of the eye has already revolutionized the field of ophthalmology [15]. In the context of skin imaging, OCT has emerged as a powerful tool for dermatologists and researchers alike, allowing real-time visualization of epidermal and dermal structures. A particularly useful implementation of OCT is known as OCT angiography, or OCTA, in which multiple images are acquired in rapid succession and volumetric motion contrast can be used to detect blood vessels [16]. OCT images are suitable for computational analysis to increase the signal-to-noise ratio and reduce speckle [17–19], reduce motion artifacts [20], and extract information in skin tissue that is not evident from the images themselves. For example, the optical attenuation coefficient can visualize the dermis and quantify its thickness [21,22]. Optical features including the scattering coefficient, absorption coefficient, and tissue anisotropy can also be extracted [23,24], and they are suitable for other machine learning and deep learning techniques [25].

Complementing OCT, PAI has gained prominence for its ability to combine the strengths of both optical and ultrasound imaging [26–28]. PAI operates by pulsing light directly at tissue. Chromophores in tissue absorb the light, leading to thermoelastic expansion and the emission of acoustic waves. These waves are then read by ultrasound transducers and reconstructed into images. Because only chromophores emit acoustic waves, and chromophore emissions are concentration- and wavelength-dependent, PAI can be used to probe the location and concentration of a range of endogenous chromophores, including hemoglobin, melanin, and collagen, as well as exogenous contrast agents, to create detailed images of tissue vasculature and chromophore distribution. The rich absorption contrast of hemoglobin and melanin in the skin makes PAI particularly adept at visualizing blood vessels, pigmented lesions, and other structures with high optical absorption. The synergy between OCT and PAI becomes evident when considering their complementary strengths [2]. While OCT excels in providing high-resolution structural information, PAI enhances functional and molecular insights, creating a holistic approach to skin assessment. Together, these modalities offer unprecedented opportunities for early disease detection, precise treatment planning, and monitoring therapeutic outcomes.

We conducted a literature review of primary research describing OCT and PAI to characterize skin that was published before December 2023. The literature search was conducted using the terms 'photoacoustic imaging' and 'optoacoustic imaging' and 'optical coherence tomography' with 'skin imaging'. Studies were excluded if they (1) did not utilize PAI or OCT methods, (2) were on organs other than skin, (3) were not in English, or (4) were not primary research papers. Our primary source was Google Scholar, which yielded 386 total results. From these, we selected a wide range of papers demonstrating the breadth of research and clinical applications that have been demonstrated to date.

2. Application of OCT in Skin Imaging

OCT in skin imaging offers valuable insights into both normal and pathological conditions [29–44]. In the assessment of inflammatory skin diseases such as psoriasis and eczema, OCT allows the real-time visualization of morphological changes within the skin layers. OCT enables clinicians to observe alterations in epidermal thickness, identify structural anomalies, and assess the vascular network in the dermis [45–50]. This capability is instrumental in characterizing lesions and understanding the dynamic evolution of inflammatory

processes. For example, in psoriasis, OCT can delineate the hyperkeratosis and acanthosis of the epidermis, providing a detailed view of the pathophysiological changes associated with this chronic condition [51–54]. OCTA is particularly useful for imaging inflammatory dermatological conditions such as psoriasis and chronic graft-versus-host disease, where differences in microvasculature can be fairly dramatic [55]. Moreover, OCT plays a pivotal role in monitoring therapeutic responses in dermatology [56,57]. This is particularly useful for nailbed diseases where biopsies are not straightforward [58]. As clinicians strive to tailor treatments for individual patients, the ability to visualize changes at a microscopic level becomes crucial. OCT also allows for the objective assessment of treatment efficacy by tracking alterations in skin architecture over time. This is particularly relevant in conditions like atopic dermatitis [51,59–63], where treatment outcomes can manifest as changes to epidermal thickness, inflammation, and barrier integrity. The real-time feedback provided by OCT aids clinicians in making informed decisions about treatment adjustments, ensuring optimal patient care. The utility of OCT extends beyond diagnosis and treatment monitoring to the realm of procedural guidance. In dermatological procedures such as skin biopsies, the precise localization of target areas is important. OCT facilitates this process by offering real-time visualization of the skin layers, assisting clinicians in identifying regions of interest with a high degree of accuracy [64–67]. This not only enhances the diagnostic yield of biopsies but also minimizes the invasiveness of the procedure. The non-destructive nature of OCT is a key advantage in dermatology, allowing for repeated imaging sessions without compromising tissue integrity. This longitudinal capability is invaluable in studying disease progression and understanding the long-term effects of therapeutic interventions [68–70]. Longitudinal OCT imaging in chronic skin conditions, such as scleroderma or chronic wounds, provides a dynamic portrait of changes in tissue morphology, aiding researchers in unraveling the complexities of these disorders [71–73]. OCT aids in the early detection and characterization of skin cancers, offering detailed insights into lesion morphology, thickness, and depth [74–80]. Particularly valuable in non-melanoma skin cancers like basal cell carcinoma and squamous cell carcinoma, OCT assists clinicians in assessing tumor margins and guiding treatment decisions [76,78,79,81–95]. Its non-invasive nature and ability to capture real-time images make OCT a valuable tool for dermatologists, contributing to more accurate diagnostics and improved management of skin cancer patients. In the research arena, OCT has become an indispensable tool for advancing our understanding of skin pathophysiology. Its ability to capture high-resolution, cross-sectional images enables researchers to explore nuances in cellular and tissue structures. OCT extends its reach to the assessment of nail disorders, providing detailed imaging of the nail plate and bed [52,54,96–99]. Moreover, OCT has been used in characterizing cutaneous vasculature, guiding interventions for conditions such as hemangiomas and port-wine stains [100]. Additionally, OCT plays a role in investigating novel therapeutic approaches, providing researchers with a means to visualize the impact of experimental treatments on skin structures.

Examples of the use of OCT skin and nail imaging for disease diagnosis and treatment monitoring are shown in Figure 1. In Figure 1a, Ha-Wissel et al. demonstrate through cross-sectional and *en face* OCTA images some differences in epidermal thickness, vascular density, and plexus depth that can be used for disease diagnosis and differentiation [62]. Figure 1b, from the same report, shows through cross-sectional and *en face* imaging the efficacy of a specific biologic therapy for atopic dermatitis over the course of a year (t = weeks). In Figure 1c, Gambichler et al. compare the ability of histopathology and OCT to detect basal cell carcinomas [57]. Nail pathologies, whether inflammatory disease or cancerous lesions are suspected, are particularly difficult to biopsy and lead to significant morbidity and long recovery times. In Figure 1d, Saleah et al. show the use of cross-sectional OCT imaging of an onychomycosis-affected toenail to assess morphological changes and treatment efficacy [58]. Waibel et al. demonstrate the capability of OCT to visualize port-wine birthmarks and hemangiomas in Figure 1e [100]. Figure 1f shows a report by Glinos et al. of a comparison of the use of OCT and histopathology for assessment of wound healing, a very significant

morbidity for seniors and persons with diabetes [101]. From a cosmetic perspective, the ability of OCT to assess epidermal thickness and skin architecture means that OCT can be used to evaluate the efficacy of many skin aesthetic procedures [102].
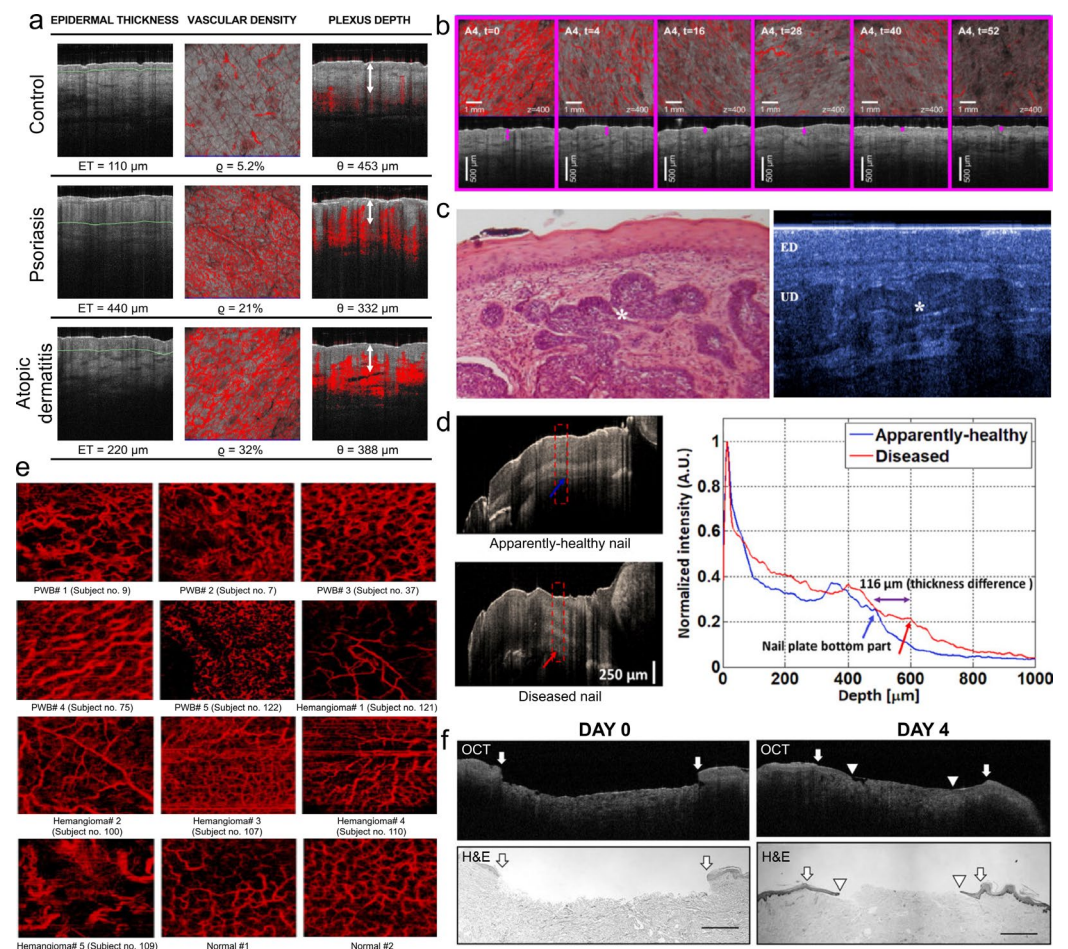
Figure 1. Examples of applications of OCT and OCTA imaging. (**a**) Some characteristics quantifiable by OCT include epidermal thickness, vascularity, and plexus depth. Image reproduced with permission from [62]. (**b**) Monitoring efficacy of biologic therapy in patient with atopic dermatitis (t = weeks). Image reproduced with permission from [62]. (**c**) Basal cell carcinomas identified by histopathology (**left**) or non-invasive OCT (**right**) showing multiple tumor lobules. Image reproduced with permission from [57]. (**d**) Cross-sectional images of healthy and diseased toenail, detecting differences in nail thickness. Image reproduced with permission from [58]. (**e**) En face images showing cutaneous vasculature of port-wine birthmarks (PWBs) and hemangiomas compared with normal skin. Image reproduced with permission from [100]. (**f**) Quantifying changes in wound healing by OCT and histopathology. Arrows indicate the initial wound edge, arrowheads indicate edge of migrating epithelial tongue. Image reproduced with permission from [101].

A major refinement in OCT imaging includes line-field confocal OCT (LC-OCT), in which light is focused to acquire only a fraction of the A-line per sweep (e.g., a confocal volume), leading to a greatly increased lateral resolution, down to ~1 μm [11]. The trade-off is that while LC-OCT can produce 3D volumes, its penetration depth is limited to the papillary dermis, missing deeper parts of tumors (~500 μm per report) [103]. Another advanced use of OCT is optical coherence elastography (OCE), in which OCT is acquired while stimulating or perturbing tissue, enabling analysis of tissue stiffness [12,13]. Polarization-sensitive OCT (PS-OCT) can measure tissue anisotropy and is especially useful for mapping collagen [14]. One group has collected data on the detection of elastic anisotropy using a combination of micro-tapping OCE with PS-OCT [104], in a small model

of healthy volunteers, including analysis of scar tissue. They found that the collagen fibers in healed scar tissue had an increased density and higher elastic moduli than healthy skin. Another way to quantify tissue composition is photothermal OCT (PT-OCT), in which skin is simultaneously illuminated with OCT and intensity-modulated photothermal lasers. The modulation establishes a thermal wave field, from which thermo-mechanical properties of the media can be inferred based on changes in the phase of the OCT signal as the lasers are varied [105], but this technology for use with endogenous imaging agents (collagen, lipids, melanin) is still in the early stages of being developed. However, PT-OCT coupled with gallic acid-tyrosine carbon dots, which are exogenous agents with high photothermal conversion efficiency, has been proposed for post-operative wound management for the prevention of microbial infection in a mouse skin wound model [106]. Limitations and challenges of OCT in skin imaging are important factors to consider in the progress of this imaging technique [107–110]. One limitation is the depth penetration of OCT, which restricts its ability to visualize deeper structures in the skin even with performing enhancement postprocessing algorithms [17,21,29,31,111–125]. Additionally, motion artifacts can affect image quality, especially in areas of the body prone to movement. Another challenge is the interpretation of OCT images, as complex structures can sometimes be difficult to interpret accurately. Furthermore, the cost and availability of OCT systems can be a limitation, restricting its widespread use in clinical practice. Finally, there remains a need for standardized protocols and guidelines for OCT imaging in dermatology to ensure consistency and reliability across different healthcare settings. Addressing these limitations and challenges will be crucial in advancing the field of OCT imaging in dermatology and improving its clinical utility.

3. Application of Photoacoustic Imaging (PAI) for Skin Imaging

In addition to many other applications [126–131], one significant application of PAI in skin imaging is its ability to visualize and characterize pigmented lesions. Melanin, the major pigment in the skin, strongly absorbs laser light, leading to the generation of photoacoustic signals. This property is particularly advantageous in the detection and analysis of pigmented skin lesions, such as melanomas. PAI allows for the differentiation between melanin-rich lesions and surrounding tissues, providing information about the depth and distribution of pigmentation [132–141]. This can aid clinicians in early melanoma detection and in distinguishing benign from malignant lesions [142]. Furthermore, PAI is instrumental in studying hemoglobin and blood vessel distribution in the skin. Hemoglobin exhibits strong absorption in the visible and near-infrared spectrum, allowing PAI to provide detailed information about blood vessel networks and oxygenation levels. This is particularly relevant in dermatology for assessing conditions such as vascular malformations, hemangiomas, and inflammatory skin disorders [143,144]. The capability to visualize and quantify blood perfusion in the skin enhances diagnostic accuracy and aids in treatment planning. In fact, a recent study was able to assess dermal microvasculature for the purpose of staging diabetes by relating the loss of dermal microvasculature with the increased likelihood of other, system diabetic complications including the extent of diabetic neuropathy and even atherosclerosis [145]. In addition to its morphological imaging capabilities, PAI can be employed for functional imaging in the skin. For instance, it enables the assessment of oxygen saturation levels in blood vessels, offering insights into tissue oxygenation. This is critical in conditions where alterations in oxygenation play a role, such as in wound healing or peripheral vascular diseases. PAI can contribute to a comprehensive understanding of tissue physiology, guiding therapeutic interventions and monitoring treatment responses. Moreover, the potential for molecular imaging is an exciting aspect of PAI in dermatology. By utilizing contrast agents or specific wavelengths that target molecular markers, researchers can visualize and characterize molecular changes associated with skin diseases [146–148]. This capability holds promise for early diagnosis and personalized treatment strategies, particularly in the context of skin cancer and inflammatory disorders. The FDA has approved several organic dyes for such applications,

including methylene blue and indocyanine green, which have been used experimentally in animal models and in human studies [149,150]. The versatility of PAI extends to its use in guiding dermatological procedures [135,151]. For instance, during laser therapies or dermatologic surgeries, PAI can assist in the real-time monitoring of tissue responses and guide the precise delivery of therapeutic interventions [152–154]. This contributes to improved treatment outcomes and minimizes potential damage to surrounding healthy tissue. PAI's ability to assess hemoglobin concentration and oxygenation in tissue has profound implications for burn depth assessment and wound monitoring by providing real-time, multispectral imaging of tissue oxygenation, showcasing the potential of PAI in guiding wound management decisions [155–160]. PAI's ability to visualize subcutaneous structures and monitor changes in collagen and elastin content positions it as a valuable tool for guiding cosmetic procedures [161–163]. PAI further demonstrated non-invasive in vivo imaging to evaluate immune responses and antimicrobial therapy against skin infections, exemplifying the versatility of PAI in cosmetic and therapeutic applications [161–163]. One popular form of PAI for skin imaging is raster scan optoacoustic mesoscopy (RSOM) [164]. This technique can acquire information from different chromophores through multispectral imaging or through use of dual transducers tuned to different wavelengths.

In Figure 2, significant applications of PAI for skin imaging are demonstrated. He et al. compare dermatoscopic, histopathologic, and PAI imaging (cross-sectional maximum intensity projection (MIP) image of the epidermis and dermis and *en face* MIPs from the epidermis and dermis layers) of a dysplastic nevus (top) and melanoma (bottom), as shown in Figure 2a. Note the significant difference in the dermal layer of the density of surrounding tissue vessels, which is evident in both the cross-sectional and *en face* images [142]. Figure 2b shows a report by many members of the same group of the effect of hemangioma treatment [165]. As with Figure 2a, the acoustic signals are divided into two frequency bands, low (red channel) and high (green channel), and beamforming is used to generate two separate images. The composite image is generated by fusing the two channels. Separation of the signal into two channels and recombination after frequency equalization enables improved rendering of fine spatial details (high frequency) and lower-resolution skin structures (low frequency). In Figure 2c, Geisler et al. demonstrate the use of PAI for wound depth assessment and the monitoring of wound healing [166]. The two channels in Figure 2c show the total PA signal intensity (scale bar, red) and oxygen saturation of tissue (scale bar, blue to red). Oxygen saturation is computed by unmixing multispectral PA images and accounting for the different contribution of saturated and unsaturated hemoglobin to the total signal. PA can not only detect psoriasis but can also be used to calculate a psoriasis area severity index (PASI). In [167], He et al. develop a deep learning-based method for automated analysis of RSOM image volumes and use it to demonstrate psoriasis severity. Again, the signal is separated into low and high frequencies. Although not particularly noticeable *en face*, in the cross-section, the vascular distribution in the epidermis is quite prominent compared with healthy skin. Nitkunanantharajah et al. [168] demonstrate nail imaging (Figure 2e). After first showing the significantly enhanced image quality of PAI compared with capillaroscopy and dermoscopy, they show its use in detecting the autoimmune disease systemic sclerosis, where there is a clear comparison between a healthy nail and examples of a sclerotic nail displaying capillary drop out, capillaries with increased width, and angiogenic, twisted capillaries. In addition to monitoring treatment response, PAI can also monitor skin damage over time [169].
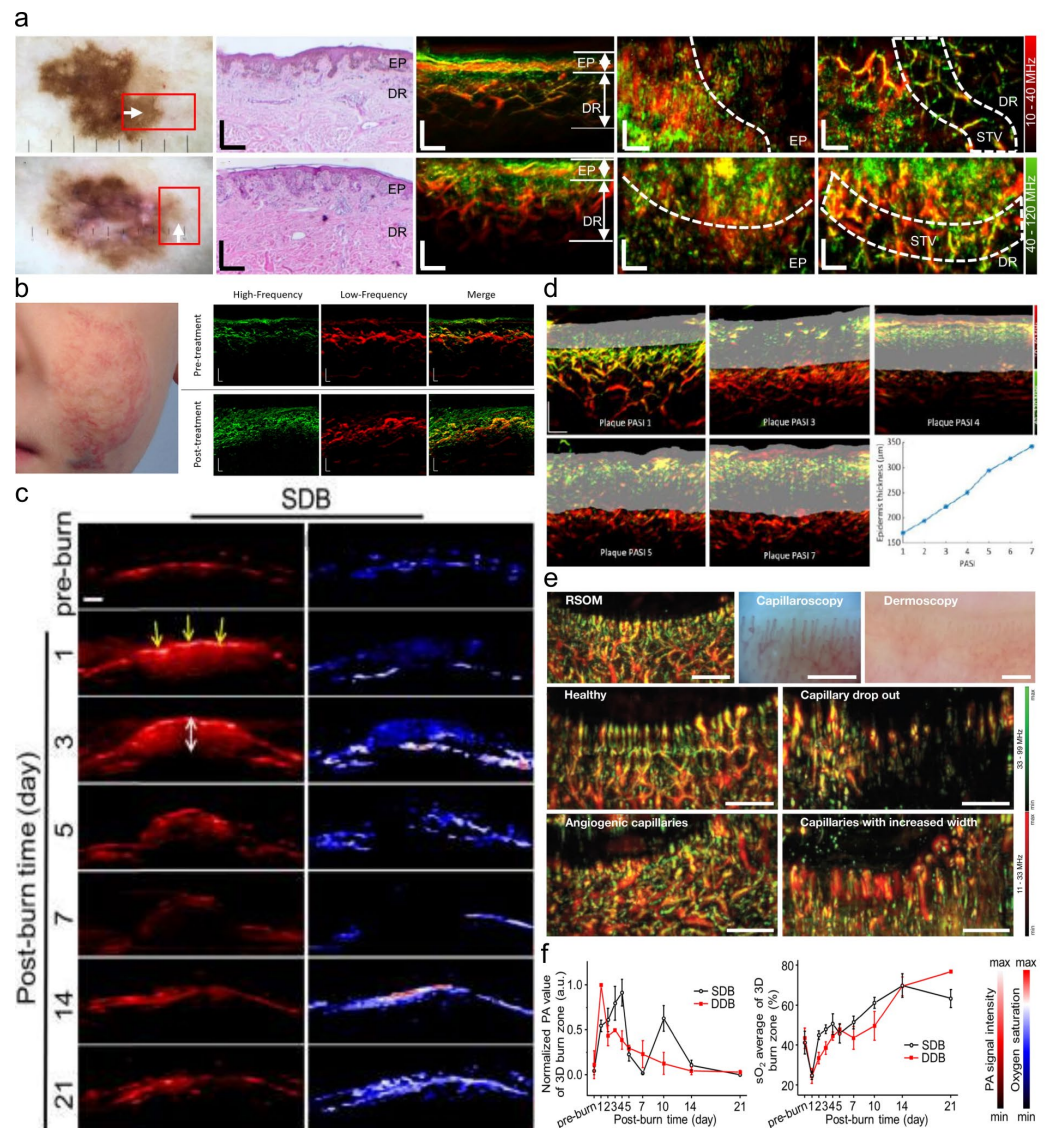
Figure 2. Selected applications of PAI for skin imaging. (**a**) Detection of melanoma and differentiation from benign dysplastic nevus. Dermoscopic, histologic, cross-sectional, and *en face* images of dysplastic nevus (**top**) and melanoma (**bottom**). EP = epidermis, DR = dermis, STV = surrounding tissue vessels. Image reproduced with permission from [142]. (**b**) Imaging hemangiomas using a combination of high (33–100 MHz) and low (10 –33 MHz) transducers by RSOM. Image reproduced with permission from [166]. (**c**) Wound depth assessment and monitoring of wound healing by quantifying PA signal intensity and oxygen saturation of tissue. Image reproduced with permission from [169]. (**d**) Psoriatic skin imaged by RSOM with depth of plaque quantified through deep learning. Psoriasis area severity index: PASI. Reproduced with permission from [167]. (**e**) Nailfold imaging by PAI shown in comparison with conventional imaging for healthy nail and systematic sclerosis. Image reproduced with permission from [168]. (**f**) Quantitative analysis of volume photoacoustic signal amplitudes (**left**) and sO₂ averages of burn zone (**right**). Image reproduced with permission from [169].

Despite its many advantages, PAI also has certain limitations and challenges for skin imaging [28], such as the necessity for safety goggles, the risk of skin damage from high-energy lasers, and the use of ultrasound gel which may not be comfortable for some kinds of lesions, but none of these limitations will stop the technology from appearing in the clinic. Moreover, the cost right now for a PAI system is far higher than those of imaging modalities such as OCT or ultrasound and is likely to be too high for a dermatology office

to use as a diagnostic-assistant device for point-of-care usage. Motion artifacts can be another limitation. Additionally, PAI has limitations in differentiating between different types of skin tissues [170]. While PAI can provide functional information about blood vessels and oxygenation levels, it may struggle to distinguish between various tissue types with similar optical properties. This can make it challenging to accurately identify specific skin structures and differentiate between healthy and diseased tissues [171]. Furthermore, the imaging speed of PAI can be a limitation in certain scenarios. PAI typically requires the acquisition of multiple images for volumetric imaging, which can increase the imaging time compared to OCT. This can be problematic for imaging moving structures or for real-time imaging applications. Finally, the availability and accessibility of PAI systems in clinical practice remain a challenge. PAI is still a relatively new and evolving technology, and its widespread adoption in dermatological practice may be limited by the availability of specialized equipment and trained personnel [171].

4. Application of Multimodal Skin Imaging Systems

Both OCT and PAI have significant strengths for skin imaging, but they also have limitations. One way to overcome such limitations is through the development of multimodal imaging systems which can extend the scope of information acquired. The natural complement for all PAI systems is ultrasound, as both can utilize the same transducer. One recent example of the combined use of PAI and ultrasound for skin lesion assessment involves a setup that integrates an acoustic mirror to enable *en face* and 3D imaging [172]. Dual PAI/US systems have been used to assess scleroderma [173], nails and the nail bed [174], burn injury [158], and other conditions. Another multimodal skin imaging system reported is a concurrent five-modal microscopy system for resolving processes in wound healing [175]. There, researchers simultaneously captured PAI, two-photon excitation fluorescence, brightfield contrast, and second- and third-harmonic generation modalities. Hyperspectral skin imaging (HSI) is a modality that has been paired, separately, with both PAI or OCT. HSI acquires multiple skin images at narrow spectral bands and extracts structural and compositional information by changes in the spectral signature of different endogenous chromophores. In this way, HSI can reveal changes in cell composition and structural changes, although it cannot image very deeply. A combined PA-HSI system has been proposed for imaging melanoma and cutaneous squamous cell carcinomas from the same system [176]. A combined OCT-HSI system has also been proposed to take advantage of structural information gleaned from OCT systems and the functional information obtained through HSI analysis [177].

Given the highly complementary nature of OCT and PAI systems, a number of research groups have explored the use of multimodal PAI/OCT systems for skin imaging [3,178,178–180]. Dual systems have the potential to overcome some of the limitations of each individual system [2]. The dual systems are typically implemented using a Fabry–Perot interferometer for PA pulse scanning and a typical swept-source OCT [178], although it has been implemented with a switchable sensor head for a dual-modality system, which, the authors claim, greatly improves OCT sensitivity [3]. The use of both techniques enables the imaging of both the microvasculature in the papillary dermis (through OCTA) and deeper vasculature (through PAI) [2]. Figure 3 shows PAI/OCTA images of the same regions of skin at the same depth, acquired using such a system. In Figure 3a, a 3D projection of healthy skin showing vasculature is presented [178]. Figure 3b shows a melanocytic lesion captured by PAI/OCTA [3]. In Figure 3c, a mouse ear is imaged before and after a burn wound [3]. There, the PAI and OCTA show changes in vasculature, while OCT demonstrates structural loss of the dermal epidermal junction. Another reported multimodal imaging setup combines OCT and PA with Raman spectroscopy [181]. In a preliminary study, the Raman signal, collected via the OCT scanning lens, was able to identify distinctive differences between normal skin and melanomas to complement the PAI/OCT results.
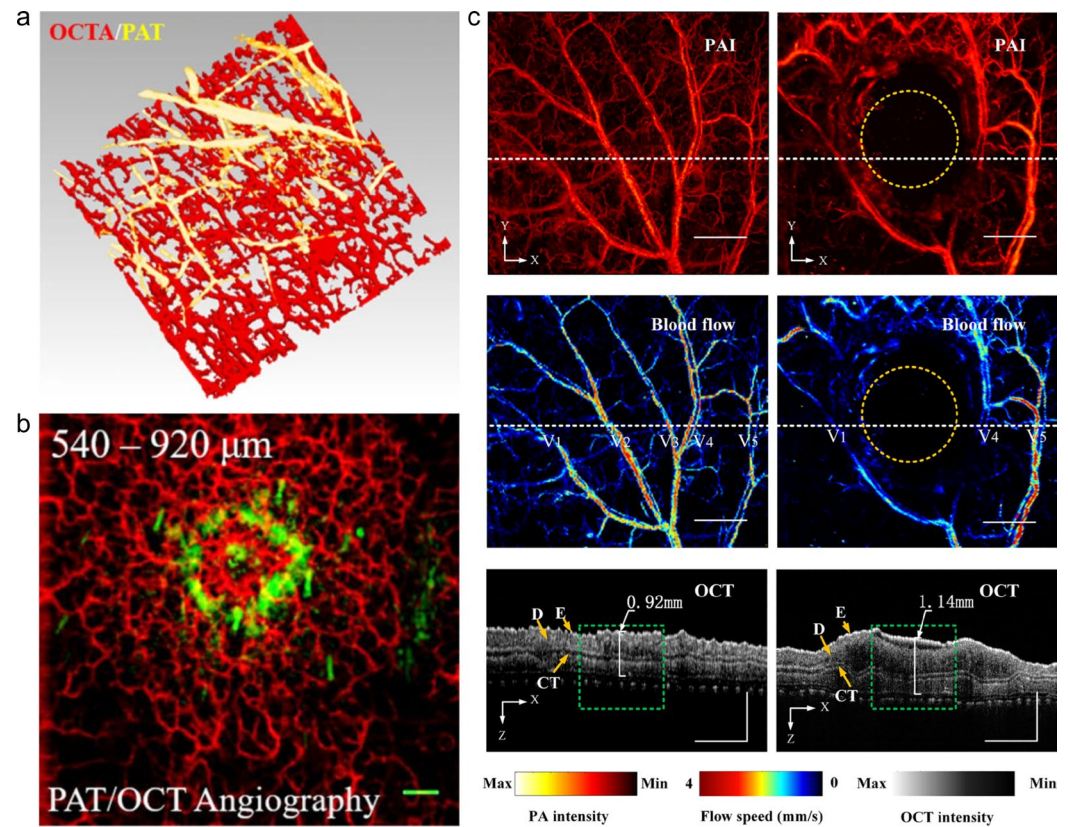
Figure 3. Examples of combined PAI/OCTA and OCT imaging. (**a**) Healthy skin, reproduced from [178]; (**b**) image of melanocytic lesion, with OCT in red and PAT in green, reproduced from [3]; (**c**) imaging of mouse ear before and after a burn showing PAI (**top row**), OCTA en face (**middle row**), and OCT cross-section (through the white dashed line) (**bottom row**). OCT shows structural changes while PAI and OCTA show loss of blood flow in burned region. Reproduced from [182].

5. Discussion and Conclusions

Recent advances in OCT and PAI have enabled a more comprehensive understanding of skin pathologies. OCT provides high-resolution (~2–10 μm axial, 1–10 μm lateral) [11,183,184], non-contact cross-sectional imaging of the skin and has found applications in dermatology primarily for diagnosing and monitoring non-melanoma skin cancers, evaluating skin aging, and assessing inflammatory skin diseases and wound healing. The depth of penetration of OCT is limited to the epidermis and part way into the dermis. PAI, on the other hand, offers functional and molecular imaging capabilities, enabling the identification of specific skin components and biomarkers. The depth of penetration includes the epidermis, dermis, and sub-dermis vasculature. Table 1 identifies the use of OCT and PAI for the diagnosis and monitoring of the therapeutic efficacy of specific clinical conditions and other dermatological uses.

Although both techniques have their limitations and challenges, their complementary nature expands the clinical potential of both modalities in the field of dermatology.

Table 1. Applications of OCT and PAI for skin imaging by condition or usage.

Condition	OCT	PAI
Psoriasis, eczema, and other inflammatory conditions	Changes in epidermal thickness, structural anomalies, alterations in dermal vascular network [45–50,55,185].	Changes in vascularity [143,144,186].
Atopic dermatitis treatment efficacy	Changes in skin architecture and dermal vascular network over time [51,59–63,187].	Changes in vascularity [188,189].
Hyperkeratosis and acanthosis of the epidermis	Changes in skin architecture [51–54].	
Non-melanoma skin cancers	Detection and identification of tumor margins [76,79,81–93].	Changes in vascularity, oxygenation, melanin [190,191].
Nail disorders	Difficult-to-biopsy information on nail plate and bed [52,54,96–99].	Changes in blood oxygenation and collagen content [174].
Hemangiomas and port-wine stains	Disordered vasculature [100].	Changes in vascularity [143,144].
Scleroderma and skin involvement in systemic sclerosis	Changes in skin architecture, skin fibrosis [71–73,192,193].	
Burn assessment	Tissue architecture, dermal vascularity [22].	Vascularity and angiogenesis [156,157,169].
Characterization of pigmented lesions and melanoma	Using machine learning/deep learning analysis [23,194].	Describes depth and distribution of pigmentation [132–142].
Wound depth assessment, healing, and peripheral vascular diseases	Skin architecture, mechanical properties [195,196].	Assessment of oxygen saturation levels in blood vessels [155–160,166].
Staging diabetes progression and potential for complications		Changes in dermal microvasculature [145].
Preparation for skin biopsies and guiding dermatological procedures	Detection of regions of interest through structural changes [64–67].	Use vascularity, melanin location for guidance [135,151–154].
Guiding delivery of therapeutic interventions and real-time tissue response		Observation of molecular changes associated with skin disease, including with the use of dyes [146–150,152–154,197].
Guiding cosmetic procedures	Assessment of skin architecture can evaluate the efficacy of many skin aesthetic procedures [102].	Assess collagen and elastin content [161–163].

The recent advancements in multimodal imaging techniques and the integration of artificial intelligence (AI) have further enhanced the accuracy and efficiency of skin imaging. The non-invasive imaging of skin cancer and other skin diseases has shown promising results. The clinical applications of OCT and PAI in dermatology extend beyond diagnosis, encompassing imaging-guided dermatological procedures and the monitoring of treatment efficacy. Advancements in OCT and PAI have the potential to revolutionize skin imaging. In OCT, advancements in technology have enabled higher resolution and faster image acquisition, allowing for a more detailed visualization of skin structures. These advancements have also led to the development of handheld OCT devices, increasing the accessibility of this imaging technique. PAI, on the other hand, has seen advancements in both hardware and software, resulting in improved signal detection and image quality. This has expanded the applications of PAI in dermatology, particularly in the diagnosis and monitoring of skin cancer. Moreover, the complementary nature of OCT and PAI makes them an ideal combination in skin imaging. The combined use of these techniques has shown promising results in detecting and characterizing skin diseases. However, there are still challenges to be addressed, such as the need for standardized imaging protocols, automated methods for co-registering PAI and OCT images, and the improvement in image interpretation algorithms. Despite these challenges, the potential advancements in OCT and PAI technology hold great promise for the future of skin imaging, paving the way for more accurate diagnosis and personalized treatment approaches in dermatology.

In order to further enhance the capabilities of these skin imaging techniques, it is crucial to address their existing limitations and improve accessibility. One major limitation is the depth penetration of these imaging modalities, especially in deeper layers of the skin. Efforts are being made to develop techniques that overcome this challenge by using advanced signal processing algorithms and hybrid imaging approaches. Additionally, the cost and size of OCT and PAI systems can hinder their usage in some healthcare settings. To improve accessibility, researchers are exploring the use of miniaturized and portable devices that are more affordable and can be used in point-of-care settings. Furthermore, the interpretation and analysis of OCT and PAI images can be time-consuming and require skilled expertise. Developing automated image analysis algorithms and incorporating AI techniques can greatly enhance the efficiency and accuracy of these imaging methods. By addressing these limitations and improving accessibility, OCT and PAI can become more widely used in dermatology, leading to the better diagnosis, monitoring, and treatment of various skin conditions.

Author Contributions: Conceptualization, M.Z. and K.A.; methodology, M.Z. and K.A.; software, R.M.; validation, M.Z., K.A. and R.M.; formal analysis, M.Z., A.P.S., K.A. and R.M.; investigation, M.Z.; writing—original draft preparation, M.Z., A.P.S., K.A. and R.M.; writing—review and editing, M.Z., K.A., A.P.S. and R.M.; visualization, R.M.; supervision, K.A. All authors have read and agreed to the published version of the manuscript.

References

1. Jablonski, N.G. The evolution of human skin and skin color. *Annu. Rev. Anthropol.* **2004**, *33*, 585–623. [CrossRef]
2. Liu, M.; Drexler, W. Optical coherence tomography angiography and photoacoustic imaging in dermatology. *Photochem. Photobiol. Sci.* **2019**, *18*, 945–962. [CrossRef] [PubMed]
3. Liu, M.; Chen, Z.; Zabihian, B.; Sinz, C.; Zhang, E.; Beard, P.C.; Ginner, L.; Hoover, E.; Minneman, M.P.; Leitgeb, R.A. Combined multi-modal photoacoustic tomography, optical coherence tomography (OCT) and OCT angiography system with an articulated probe for in vivo human skin structure and vasculature imaging. *Biomed. Opt. Express* **2016**, *7*, 3390–3402. [CrossRef] [PubMed]
4. Diotallevi, F.; Offidani, A. Skin, Autoimmunity and Inflammation: A Comprehensive Exploration through Scientific Research. *Int. J. Mol. Sci.* **2023**, *24*, 15857. [CrossRef] [PubMed]
5. Wassef, C.; Rao, B.K. Uses of non-invasive imaging in the diagnosis of skin cancer: An overview of the currently available modalities. *Int. J. Dermatol.* **2013**, *52*, 1481–1489. [CrossRef] [PubMed]

6. MacFarlane, D.; Shah, K.; Wysong, A.; Wortsman, X.; Humphreys, T.R. The role of imaging in the management of patients with nonmelanoma skin cancer: Diagnostic modalities and applications. *J. Am. Acad. Dermatol.* **2017**, *76*, 579–588. [CrossRef] [PubMed]

7. Bae, Y.; Nelson, J.S.; Jung, B. Multimodal facial color imaging modality for objective analysis of skin lesions. *J. Biomed. Opt.* **2008**, *13*, 064007–064008. [CrossRef]

8. Burkes, S.; Adams, D.; Hammill, A.; Chute, C.; Eaton, K.; Welge, J.; Wickett, R.; Visscher, M. Skin imaging modalities quantify progression and stage of infantile haemangiomas. *Br. J. Dermatol.* **2015**, *173*, 838–841. [CrossRef] [PubMed]

9. Halani, S.; Foster, F.S.; Breslavets, M.; Shear, N.H. Ultrasound and infrared-based imaging modalities for diagnosis and management of cutaneous diseases. *Front. Med.* **2018**, *5*, 115. [CrossRef]

10. Wilhelm, K.-P.; Elsner, P.; Berardesca, E.; Maibach, H.I. *Bioengineering of the Skin: Skin Imaging & Analysis*; CRC Press: Boca Raton, FL, USA, 2006.

11. Schuh, S.; Ruini, C.; Perwein, M.K.E.; Daxenberger, F.; Gust, C.; Sattler, E.C.; Welzel, J. Line-field confocal optical coherence tomography: A new tool for the differentiation between nevi and melanomas? *Cancers* **2022**, *14*, 1140. [CrossRef]

12. Larin, K.V.; Sampson, D.D. Optical coherence elastography–OCT at work in tissue biomechanics. *Biomed. Opt. Express* **2017**, *8*, 1172–1202. [CrossRef] [PubMed]

13. Liang, X.; Boppart, S.A. Biomechanical properties of in vivo human skin from dynamic optical coherence elastography. *IEEE Trans. Biomed. Eng.* **2010**, *57*, 953–959. [CrossRef] [PubMed]

14. Tang, P.; Kirby, M.A.; Le, N.; Li, Y.; Zeinstra, N.; Lu, G.N.; Murry, C.E.; Zheng, Y.; Wang, R.K. Polarization sensitive optical coherence tomography with single input for imaging depth-resolved collagen organizations. *Light: Sci. Appl.* **2021**, *10*, 237. [CrossRef] [PubMed]

15. Zeppieri, M.; Marsili, S.; Enaholo, E.S.; Shuaibu, A.O.; Uwagboe, N.; Salati, C.; Spadea, L.; Musa, M. Optical Coherence Tomography (OCT): A Brief Look at the Uses and Technological Evolution of Ophthalmology. *Medicina* **2023**, *59*, 2114. [CrossRef] [PubMed]

16. Xu, J.; Song, S.; Men, S.; Wang, R.K. Long ranging swept-source optical coherence tomography-based angiography outperforms its spectral-domain counterpart in imaging human skin microcirculations. *J. Biomed. Opt.* **2017**, *22*, 116007. [CrossRef] [PubMed]

17. Eybposh, M.H.; Turani, Z.; Mehregan, D.; Nasiriavanaki, M. Cluster-based filtering framework for speckle reduction in OCT images. *Biomed. Opt. Express* **2018**, *9*, 6359–6373. [CrossRef] [PubMed]

18. Avanaki, M.; Laissue, P.P.; Hojjatoleslami, A. De-noising speckled optical coherence tomography images using an algorithm based on artificial neural network. *J. Neurosci. Neuroeng.* **2013**, *2*, 347–352. [CrossRef]

19. Rahaman, J.; Lukas, B.; May, J.; Puyana, C.; Tsoukas, M.; Avanaki, K. *A Fast Normalization and Despeckled Method for Skin Optical Coherence Tomography Image via Deep Learning*; SPIE: Bellingham, WA, USA, 2023; Volume 12352.

20. Cheng, Y.; Chu, Z.; Wang, R.K. Robust three-dimensional registration on optical coherence tomography angiography for speckle reduction and visualization. *Quant. Imaging Med. Surg.* **2021**, *11*, 879–894. [CrossRef] [PubMed]

21. Xu, Q.; May, J.; Smith, J.; Fakhoury, J.; Daveluy, S.; Chen, W.; Avanaki, K. Study of variation of attenuation coefficient in different skin color and age groups using optical coherence tomography. In Proceedings of the Photonics in Dermatology and Plastic Surgery 2022, San Francisco, CA, USA, 20–24 February 2022; p. PC119340P.

22. Lu, J.; Deegan, A.J.; Cheng, Y.; Liu, T.; Zheng, Y.; Mandell, S.P.; Wang, R.K. Application of OCT-derived attenuation coefficient in acute burn-damaged skin. *Lasers Surg. Med.* **2021**, *53*, 1192–1200. [CrossRef] [PubMed]

23. Turani, Z.; Fatemizadeh, E.; Blumetti, T.; Daveluy, S.; Moraes, A.F.; Chen, W.; Mehregan, D.; Andersen, P.E.; Nasiriavanaki, M. Optical Radiomic Signatures Derived from Optical Coherence Tomography Images Improve Identification of Melanoma. *Cancer Res.* **2019**, *79*, 2021–2030. [CrossRef] [PubMed]

24. Turani, Z.; Fatemizadeh, E.; Blumetti, T.; Daveluy, S.; Moraes, A.F.; Chen, W.; Mehregan, D.; Andersen, P.E.; Avanaki, K. Melanoma detection using quantitative analysis of optical coherence tomography images. In Proceedings of the Optical Interactions with Tissue and Cells XXXII, Online, 6–11 March 2021; p. 116400T.

25. Lin, C.-H.; Lukas, B.E.; Rajabi-Estarabadi, A.; May, J.R.; Pang, Y.; Puyana, C.; Tsoukas, M.; Avanaki, K. Rapid measurement of epidermal thickness in OCT images of skin. *Sci. Rep.* **2024**, *14*, 2230. [CrossRef] [PubMed]

26. Fujimoto, J.G.; Schmitt, J.M. Principles of OCT. In *Optical Coherence Tomography in Cardiovascular Research*; CRC Press: Boca Raton, FL, USA, 2007; pp. 35–50.

27. Aumann, S.; Donner, S.; Fischer, J.; Müller, F. Optical coherence tomography (OCT): Principle and technical realization. In *High Resolution Imaging in Microscopy and Ophthalmology: New Frontiers in Biomedical Optics*; Springer: Berlin/Heidelberg, Germany, 2019; pp. 59–85.

28. Li, D.; Humayun, L.; Vienneau, E.; Vu, T.; Yao, J. Seeing through the skin: Photoacoustic tomography of skin vasculature and beyond. *JID Innov.* **2021**, *1*, 100039. [CrossRef] [PubMed]

29. Xu, Q. *The Advanced Applications for Optical Coherence Tomography in Skin Imaging*; Wayne State University: Detroit, MI, USA, 2021.

30. Fayyaz, Z.; Mohammadian, N.; Reza Rahimi Tabar, M.; Manwar, R.; Avanaki, K. A comparative study of optimization algorithms for wavefront shaping. *J. Innov. Opt. Health Sci.* **2019**, *12*, 1942002. [CrossRef]

31. Forouzandeh, M.; Rajabi-Estarabadi, A.; Williams, N.M.; Avanaki, M.R.; Nouri, K. The efficacy and morphological effects of hydrogen peroxide 40% topical solution for the treatment of seborrheic keratoses, evaluated by dynamic optical coherence tomography. *Ski. Res. Technol.* **2020**, *26*, 142–145. [CrossRef] [PubMed]

32. Jalilian, E.; Xu, Q.; Horton, L.; Fotouhi, A.; Reddy, S.; Manwar, R.; Daveluy, S.; Mehregan, D.; Gelovani, J.; Avanaki, K. Contrast-enhanced optical coherence tomography for melanoma detection: An in vitro study. *J. Biophotonics* **2020**, *13*, e201960097. [CrossRef] [PubMed]

33. Avanaki, M.R.; Podoleanu, A. En-face time-domain optical coherence tomography with dynamic focus for high-resolution imaging. *J. Biomed. Opt.* **2017**, *22*, 056009. [CrossRef] [PubMed]

34. Tes, D.; Aber, A.; Zafar, M.; Horton, L.; Fotouhi, A.; Xu, Q.; Moiin, A.; Thompson, A.D.; Moraes Pinto Blumetti, T.C.; Daveluy, S. Granular cell tumor imaging using optical coherence tomography. *Biomed. Eng. Comput. Biol.* **2018**, *9*, 1179597218790250. [CrossRef]

35. Avanaki, M.R.; Hojjatoleslami, A.; Sira, M.; Schofield, J.B.; Jones, C.; Podoleanu, A.G. Investigation of basal cell carcinoma using dynamic focus optical coherence tomography. *Appl. Opt.* **2013**, *52*, 2116–2124. [CrossRef] [PubMed]

36. Avanaki, M.R.; Hojjat, A.; Podoleanu, A.G. Investigation of computer-based skin cancer detection using optical coherence tomography. *J. Mod. Opt.* **2009**, *56*, 1536–1544. [CrossRef]

37. Xu, Q.; Jalilian, E.; Fakhoury, J.W.; Manwar, R.; Michniak-Kohn, B.; Elkin, K.B.; Avanaki, K. Monitoring the topical delivery of ultrasmall gold nanoparticles using optical coherence tomography. *Ski. Res. Technol.* **2020**, *26*, 263–268. [CrossRef]

38. Lee, J.; Benavides, J.; Manwar, R.; Puyana, C.; May, J.; Tsoukas, M.; Avanaki, K. Noninvasive imaging exploration of phacomatosis pigmentokeratotica using high-frequency ultrasound and optical coherence tomography: Can biopsy of PPK patients be avoided? *Ski. Res. Technol.* **2023**, *29*, e13279. [CrossRef] [PubMed]

39. Avanaki, K.; Andersen, P. Oct Radiomic Features for Differentiation of Early Malignant Melanoma from Benign Nevus. Google Patents: 2020 Patent no. US20200359887, 19 November 2020.

40. Avanaki, K.; Andersen, P.E. Optical Coherence Tomography for Melanoma Detection. In *New Technologies in Dermatological Science and Practice*; CRC Press: Boca Raton, FL, USA, 2021; pp. 47–58.

41. Turani, Z.; Fatemizadeh, E.; Blumetti, T.; Daveluy, S.; Moraes, A.F.; Chen, W.; Mehregan, D.; Andersen, P.E.; Nasiriavanaki, M. Optical radiomic signatures derived from OCT images to improve identification of melanoma. In Proceedings of the European Conference on Biomedical Optics, Munich, Germany, 20–24 June 2021; p. 11078_23.

42. Lukas, B.; May, J.R.; Tsoukas, M.; Avanaki, K. Skin cancer detection using optical coherence tomography. In *Optical Spectroscopy And Imaging For Cancer Diagnostics: Fundamentals, Progress, and Challenges*; World Scientific: Singapore, 2023; pp. 473–495.

43. Xu, Q.; Adabi, S.; Clayton, A.; Daveluy, S.; Mehregan, D.; Nasiriavanaki, M. Swept-Source Optical Coherence Tomography–Supervised Biopsy. *Dermatol. Surg.* **2018**, *44*, 768–775. [CrossRef] [PubMed]

44. Adabi, S.; Hosseinzadeh, M.; Noei, S.; Conforto, S.; Daveluy, S.; Clayton, A.; Mehregan, D.; Nasiriavanaki, M. Universal in vivo textural model for human skin based on optical coherence tomograms. *Sci. Rep.* **2017**, *7*, 17912. [CrossRef] [PubMed]

45. Gambichler, T.; Boms, S.; Stücker, M.; Kreuter, A.; Moussa, G.; Sand, M.; Altmeyer, P.; Hoffmann, K. Epidermal thickness assessed by optical coherence tomography and routine histology: Preliminary results of method comparison. *J. Eur. Acad. Dermatol. Venereol.* **2006**, *20*, 791–795. [CrossRef] [PubMed]

46. Gambichler, T.; Matip, R.; Moussa, G.; Altmeyer, P.; Hoffmann, K. In vivo data of epidermal thickness evaluated by optical coherence tomography: Effects of age, gender, skin type, and anatomic site. *J. Dermatol. Sci.* **2006**, *44*, 145–152. [CrossRef] [PubMed]

47. Mogensen, M.; Morsy, H.A.; Thrane, L.; Jemec, G.B.E. Morphology and Epidermal Thickness of Normal Skin Imaged by Optical Coherence Tomography. *Dermatology* **2008**, *217*, 14–20. [CrossRef] [PubMed]

48. Josse, G.; George, J.; Black, D. Automatic measurement of epidermal thickness from optical coherence tomography images using a new algorithm. *Ski. Res. Technol.* **2011**, *17*, 314–319. [CrossRef] [PubMed]

49. Weissman, J.; Hancewicz, T.; Kaplan, P. Optical coherence tomography of skin for measurement of epidermal thickness by shapelet-based image analysis. *Opt. Express* **2004**, *12*, 5760–5769. [CrossRef] [PubMed]

50. Olsen, J.; Gaetti, G.; Grandahl, K.; Jemec, G.B.E. Optical coherence tomography quantifying photo aging: Skin microvasculature depth, epidermal thickness and UV exposure. *Arch. Dermatol. Res.* **2022**, *314*, 469–476. [CrossRef]

51. Welzel, J.; Bruhns, M.; Wolff, H.H. Optical coherence tomography in contact dermatitis and psoriasis. *Arch. Dermatol. Res.* **2003**, *295*, 50–55. [CrossRef] [PubMed]

52. Aydin, S.Z.; Ash, Z.; Del Galdo, F.; Marzo-Ortega, H.; Wakefield, R.J.; Emery, P.; McGonagle, D. Optical Coherence Tomography: A New Tool to Assess Nail Disease in Psoriasis? *Dermatology* **2011**, *222*, 311–313. [CrossRef] [PubMed]

53. Morsy, H.; Kamp, S.; Thrane, L.; Behrendt, N.; Saunder, B.; Zayan, H.; Elmagid, E.A.; Jemec, G.B.E. Optical coherence tomography imaging of psoriasis vulgaris: Correlation with histology and disease severity. *Arch. Dermatol. Res.* **2010**, *302*, 105–111. [CrossRef] [PubMed]

54. Aldahan, A.S.; Chen, L.L.; Fertig, R.M.; Holmes, J.; Shah, V.V.; Mlacker, S.; Hsu, V.M.; Nouri, K.; Tosti, A. Vascular features of nail psoriasis using dynamic optical coherence tomography. *Ski. Appendage Disord.* **2016**, *2*, 102–108. [CrossRef]

55. Deegan, A.J.; Talebi-Liasi, F.; Song, S.; Li, Y.; Xu, J.; Men, S.; Shinohara, M.M.; Flowers, M.E.; Lee, S.J.; Wang, R.K. Optical coherence tomography angiography of normal skin and inflammatory dermatologic conditions. *Lasers Surg. Med.* **2018**, *50*, 183–193. [CrossRef] [PubMed]

56. Ulrich, M.; Themstrup, L.; de Carvalho, N.; Manfredi, M.; Grana, C.; Ciardo, S.; Kästle, R.; Holmes, J.; Whitehead, R.; Jemec, G.B.E.; et al. Dynamic Optical Coherence Tomography in Dermatology. *Dermatology* **2016**, *232*, 298–311. [CrossRef] [PubMed]

57. Gambichler, T.; Orlikov, A.; Vasa, R.; Moussa, G.; Hoffmann, K.; Stücker, M.; Altmeyer, P.; Bechara, F.G. In vivo optical coherence tomography of basal cell carcinoma. *J. Dermatol. Sci.* **2007**, *45*, 167–173. [CrossRef] [PubMed]

58. Saleah, S.A.; Gu, Y.; Wijesinghe, R.E.; Seong, D.; Cho, H.; Jeon, M.; Kim, J. Comparative quantifications and morphological monitoring of the topical treatment approach for onychomycosis-affected in vivo toenail using optical coherence tomography: A case study. *Biomed. Signal Process. Control* **2024**, *88*, 105648. [CrossRef]

59. Byers, R.A.; Maiti, R.; Danby, S.G.; Pang, E.J.; Mitchell, B.; Carré, M.J.; Lewis, R.; Cork, M.J.; Matcher, S.J. Sub-clinical assessment of atopic dermatitis severity using angiographic optical coherence tomography. *Biomed. Opt. Express* **2018**, *9*, 2001–2017. [CrossRef] [PubMed]

60. Byers, R.A.; Maiti, R.; Danby, S.G.; Pang, E.J.; Mitchell, B.; Carré, M.J.; Lewis, R.; Cork, M.J.; Matcher, S.J. Characterizing the microcirculation of atopic dermatitis using angiographic optical coherence tomography. In *Photonics in Dermatology and Plastic Surgery*; SPIE: Bellingham, WA, USA, 2017; Volume 10037, pp. 114–122.

61. Manfredini, M.; Liberati, S.; Ciardo, S.; Bonzano, L.; Guanti, M.; Chester, J.; Kaleci, S.; Pellacani, G. Microscopic and functional changes observed with dynamic optical coherence tomography for severe refractory atopic dermatitis treated with dupilumab. *Ski. Res. Technol.* **2020**, *26*, 779–787. [CrossRef] [PubMed]

62. Ha-Wissel, L.; Yasak, H.; Huber, R.; Zillikens, D.; Ludwig, R.J.; Thaçi, D.; Hundt, J.E. Case report: Optical coherence tomography for monitoring biologic therapy in psoriasis and atopic dermatitis. *Front. Med.* **2022**, *9*, 995883. [CrossRef]

63. Boone, M.A.L.M.; Jemec, G.B.E.; Del Marmol, V. Differentiating allergic and irritant contact dermatitis by high-definition optical coherence tomography: A pilot study. *Arch. Dermatol. Res.* **2015**, *307*, 11–22. [CrossRef] [PubMed]

64. Brezinski, M.E.; Tearney, G.J.; Boppart, S.A.; Swanson, E.A.; Southern, J.F.; Fujimoto, J.G. Optical Biopsy with Optical Coherence Tomography: Feasibility for Surgical Diagnostics. *J. Surg. Res.* **1997**, *71*, 32–40. [CrossRef]

65. Kuo, W.-C.; Kim, J.; Shemonski, N.D.; Chaney, E.J.; Spillman, D.R.; Boppart, S.A. Real-time three-dimensional optical coherence tomography image-guided core-needle biopsy system. *Biomed. Opt. Express* **2012**, *3*, 1149–1161. [CrossRef] [PubMed]

66. Shostak, E.; Hariri, L.P.; Cheng, G.Z.; Adams, D.C.; Suter, M.J. Needle-based Optical Coherence Tomography to Guide Transbronchial Lymph Node Biopsy. *J. Bronchol. Interv. Pulmonol.* **2018**, *25*, 189–197. [CrossRef] [PubMed]

67. Hariri, L.P.; Mino-Kenudson, M.; Applegate, M.B.; Mark, E.J.; Tearney, G.J.; Lanuti, M.; Channick, C.L.; Chee, A.; Suter, M.J. Toward the Guidance of Transbronchial Biopsy: Identifying Pulmonary Nodules with Optical Coherence Tomography. *Chest* **2013**, *144*, 1261–1268. [CrossRef]

68. Komukai, K.; Kubo, T.; Kitabata, H.; Matsuo, Y.; Ozaki, Y.; Takarada, S.; Okumoto, Y.; Shiono, Y.; Orii, M.; Shimamura, K.; et al. Effect of Atorvastatin Therapy on Fibrous Cap Thickness in Coronary Atherosclerotic Plaque as Assessed by Optical Coherence Tomography. *J. Am. Coll. Cardiol.* **2014**, *64*, 2207–2217. [CrossRef] [PubMed]

69. Takarada, S.; Imanishi, T.; Kubo, T.; Tanimoto, T.; Kitabata, H.; Nakamura, N.; Tanaka, A.; Mizukoshi, M.; Akasaka, T. Effect of statin therapy on coronary fibrous-cap thickness in patients with acute coronary syndrome: Assessment by optical coherence tomography study. *Atherosclerosis* **2009**, *202*, 491–497. [CrossRef] [PubMed]

70. Pieper, M.; Schulz-Hildebrandt, H.; Mall, M.A.; Hüttmann, G.; König, P. Intravital microscopic optical coherence tomography imaging to assess mucus-mobilizing interventions for muco-obstructive lung disease in mice. *Am. J. Physiol. Lung Cell. Mol. Physiol.* **2020**, *318*, L518–L524. [CrossRef] [PubMed]

71. Giuseppina, A.; Sibel Zehra, A.; Concepción, C.-G.; Vasiliki, L.; Daniel, W.; Adam, M.; Richard, J.W.; Dennis, G.M.; Paul, E.; Francesco Del, G. Virtual skin biopsy by optical coherence tomography: The first quantitative imaging biomarker for scleroderma. *Ann. Rheum. Dis.* **2013**, *72*, 1845. [CrossRef]

72. Zhang, L.; Li, M.; Liu, Y.; Zhou, Q. Combining optical coherence tomography with magnetic resonance angiography and Doppler ultrasonography for clinical detection of scleroderma. *Anat. Rec.* **2020**, *303*, 3108–3116. [CrossRef]

73. Sahin-Atik, S.; Koc, F.; Akin-Sari, S.; Ozmen, M. Retinal Nerve Fiber and Optic Disc Morphology Using Spectral-Domain Optical Coherence Tomography in Scleroderma Patients. *Eur. J. Ophthalmol.* **2017**, *27*, 281–284. [CrossRef]

74. Levine, A.; Wang, K.; Markowitz, O. Optical coherence tomography in the diagnosis of skin cancer. *Dermatol. Clin.* **2017**, *35*, 465–488. [CrossRef] [PubMed]

75. di Ruffano, L.F.; Dinnes, J.; Deeks, J.J.; Chuchu, N.; Bayliss, S.E.; Davenport, C.; Takwoingi, Y.; Godfrey, K.; O'Sullivan, C.; Matin, R.N.; et al. Optical coherence tomography for diagnosing skin cancer in adults. *Cochrane Database Syst. Rev.* **2018**, *12*.

76. Rajabi-Estarabadi, A.; Bittar, J.M.; Zheng, C.; Nascimento, V.; Camacho, I.; Feun, L.G.; Nasiriavanaki, M.; Kunz, M.; Nouri, K. Optical coherence tomography imaging of melanoma skin cancer. *Lasers Med. Sci.* **2019**, *34*, 411–420. [CrossRef]

77. Mogensen, M.; Jørgensen, T.M.; Nurnberg, B.M.; Morsy, H.A.; Thomsen, J.B.; Thrane, L.; Jemec, G.B. Assessment of optical coherence tomography imaging in the diagnosis of non-melanoma skin cancer and benign lesions versus normal skin: Observer-blinded evaluation by dermatologists and pathologists. *Dermatol. Surg.* **2009**, *35*, 965–972. [CrossRef] [PubMed]

78. Alawi, S.A.; Kuck, M.; Wahrlich, C.; Batz, S.; McKenzie, G.; Fluhr, J.W.; Lademann, J.; Ulrich, M. Optical coherence tomography for presurgical margin assessment of non-melanoma skin cancer—A practical approach. *Exp. Dermatol.* **2013**, *22*, 547–551. [CrossRef] [PubMed]

79. Xiong, Y.-Q.; Mo, Y.; Wen, Y.-Q.; Cheng, M.-J.; Huo, S.-T.; Chen, X.-J.; Chen, Q. Optical coherence tomography for the diagnosis of malignant skin tumors: A meta-analysis. *J. Biomed. Opt.* **2018**, *23*, 020902. [CrossRef] [PubMed]

80. Jørgensen, T.M.; Tycho, A.; Mogensen, M.; Bjerring, P.; Jemec, G.B.E. Machine-learning classification of non-melanoma skin cancers from image features obtained by optical coherence tomography. *Ski. Res. Technol.* **2008**, *14*, 364–369. [CrossRef] [PubMed]

81. Boone, M.; Suppa, M.; Dhaenens, F.; Miyamoto, M.; Marneffe, A.; Jemec, G.; Del Marmol, V.; Nebosis, R.J.A.o.d.r. In vivo assessment of optical properties of melanocytic skin lesions and differentiation of melanoma from non-malignant lesions by high-definition optical coherence tomography. *Arch. Dermatol. Res.* **2016**, *308*, 7–20. [CrossRef] [PubMed]

82. Forsea, A.M.; Carstea, E.M.; Ghervase, L.; Giurcaneanu, C.; Pavelescu, G. Clinical application of optical coherence tomography for the imaging of non-melanocytic cutaneous tumors: A pilot multi-modal study. *J. Med. Life* **2010**, *3*, 381–389. [PubMed]

83. Wang, Y.-J.; Wang, J.-Y.; Wu, Y.-H. Application of cellular resolution full-field optical coherence tomography in vivo for the diagnosis of skin tumours and inflammatory skin diseases: A pilot study. *Dermatology* **2022**, *238*, 121–131. [CrossRef] [PubMed]

84. Calin, M.A.; Parasca, S.V.; Savastru, R.; Calin, M.R.; Dontu, S. Optical techniques for the noninvasive diagnosis of skin cancer. *J. Cancer Res. Clin. Oncol.* **2013**, *139*, 1083–1104. [CrossRef] [PubMed]

85. Wan, B.; Ganier, C.; Du-Harpur, X.; Harun, N.; Watt, F.M.; Patalay, R.; Lynch, M.D. Applications and future directions for optical coherence tomography in dermatology. *Br. J. Dermatol.* **2021**, *184*, 1014–1022. [CrossRef] [PubMed]

86. Hussain, A.A.; Themstrup, L.; Nürnberg, B.M.; Jemec, G.B.E. Adjunct use of optical coherence tomography increases the detection of recurrent basal cell carcinoma over clinical and dermoscopic examination alone. *Photodiagnosis Photodyn. Ther.* **2016**, *14*, 178–184. [CrossRef] [PubMed]

87. Patil, C.A.; Kirshnamoorthi, H.; Ellis, D.L.; van Leeuwen, T.G.; Mahadevan-Jansen, A. A clinical instrument for combined raman spectroscopy-optical coherence tomography of skin cancers. *Lasers Surg. Med.* **2011**, *43*, 143–151. [CrossRef] [PubMed]

88. Cinotti, E.; Brunetti, T.; Cartocci, A.; Tognetti, L.; Suppa, M.; Malvehy, J.; Perez-Anker, J.; Puig, S.; Perrot, J.L.; Rubegni, P. Diagnostic Accuracy of Line-Field Confocal Optical Coherence Tomography for the Diagnosis of Skin Carcinomas. *Diagnostics* **2023**, *13*, 361. [CrossRef] [PubMed]

89. Boone, M.; Suppa, M.; Miyamoto, M.; Marneffe, A.; Jemec, G.; Del Marmol, V. In vivo assessment of optical properties of basal cell carcinoma and differentiation of BCC subtypes by high-definition optical coherence tomography. *Biomed. Opt. Express* **2016**, *7*, 2269–2284. [CrossRef]

90. Patil, C.; Krishnamoorthi, H.; Ellis, D.; van Leeuwen, T.; Mahadevan-Jansen, A. *A Clinical Probe for Combined Raman Spectroscopy-Optical Coherence Tomography (RS-OCT) of the Skin Cancers*; SPIE: Bellingham, WA, USA, 2010; Volume 7548.

91. Hamdoon, Z.; Jerjes, W.; Upile, T.; McKenzie, G.; Jay, A.; Hopper, C. Optical coherence tomography in the assessment of suspicious oral lesions: An immediate ex vivo study. *Photodiagnosis Photodyn. Ther.* **2013**, *10*, 17–27. [CrossRef] [PubMed]

92. Saboowala, H.K. Understanding the Principles of Skin Optical Coherence Tomography (OCT), Technology & Clinical Applications: An Overview. 2022. Available online: https://books.google.co.jp/books?id=7EBnEAAAQBAJ&printsec=frontcover&source=gbs_ge_summary_r&cad=0#v=onepage&q&f=false (accessed on 6 February 2024).

93. Panzarella, V.; Buttacavoli, F.; Gambino, A.; Capocasale, G.; Di Fede, O.; Mauceri, R.; Rodolico, V.; Campisi, G. Site-Coded Oral Squamous Cell Carcinoma Evaluation by Optical Coherence Tomography (OCT): A Descriptive Pilot Study. *Cancers* **2022**, *14*, 5916. [CrossRef] [PubMed]

94. Mesa, K.J.; Selmic, L.E.; Pande, P.; Monroy, G.L.; Reagan, J.; Samuelson, J.; Driskell, E.; Li, J.; Marjanovic, M.; Chaney, E.J.; et al. Intraoperative optical coherence tomography for soft tissue sarcoma differentiation and margin identification. *Lasers Surg. Med.* **2017**, *49*, 240–248. [CrossRef]

95. Ha, R.; Friedlander, L.C.; Hibshoosh, H.; Hendon, C.; Feldman, S.; Ahn, S.; Schmidt, H.; Akens, M.K.; Fitzmaurice, M.; Wilson, B.C.; et al. Optical Coherence Tomography: A Novel Imaging Method for Post-lumpectomy Breast Margin Assessment—A Multi-reader Study. *Acad. Radiol.* **2018**, *25*, 279–287. [CrossRef] [PubMed]

96. Abignano, G.; Laws, P.; Del Galdo, F.; Marzo-Ortega, H.; McGonagle, D. Three-dimensional nail imaging by optical coherence tomography: A novel biomarker of response to therapy for nail disease in psoriasis and psoriatic arthritis. *Clin. Exp. Dermatol.* **2019**, *44*, 462–465. [CrossRef] [PubMed]

97. Aydin, S.Z.; Castillo-Gallego, C.; Ash, Z.R.; Abignano, G.; Marzo-Ortega, H.; Wittmann, M.; Del Galdo, F.; McGonagle, D. Potential Use of Optical Coherence Tomography and High-Frequency Ultrasound for the Assessment of Nail Disease in Psoriasis and Psoriatic Arthritis. *Dermatology* **2013**, *227*, 45–51. [CrossRef] [PubMed]

98. Sattler, E.; Kaestle, R.; Rothmund, G.; Welzel, J. Confocal laser scanning microscopy, optical coherence tomography and transonychial water loss for in vivo investigation of nails. *Br. J. Dermatol.* **2012**, *166*, 740–746. [CrossRef] [PubMed]

99. Saleah, S.A.; Kim, P.; Seong, D.; Wijesinghe, R.E.; Jeon, M.; Kim, J. A preliminary study of post-progressive nail-art effects on in vivo nail plate using optical coherence tomography-based intensity profiling assessment. *Sci. Rep.* **2021**, *11*, 666. [CrossRef] [PubMed]

100. Waibel, J.S.; Holmes, J.; Rudnick, A.; Woods, D.; Kelly, K.M. Angiographic optical coherence tomography imaging of hemangiomas and port wine birthmarks. *Lasers Surg. Med.* **2018**, *50*, 718–726. [CrossRef] [PubMed]

101. Glinos, G.D.; Verne, S.H.; Aldahan, A.S.; Liang, L.; Nouri, K.; Elliot, S.; Glassberg, M.; Cabrera DeBuc, D.; Koru-Sengul, T.; Tomic-Canic, M. Optical coherence tomography for assessment of epithelialization in a human ex vivo wound model. *Wound Repair Regen.* **2017**, *25*, 1017–1026. [CrossRef] [PubMed]

102. Kislevitz, M.; Akgul, Y.; Wamsley, C.; Hoopman, J.; Kenkel, J. Use of optical coherence tomography (OCT) in aesthetic skin assessment—A short review. *Lasers Surg. Med.* **2020**, *52*, 699–704. [CrossRef] [PubMed]

103. Ruini, C.; Schuh, S.; Sattler, E.; Welzel, J. Line-field confocal optical coherence tomography—Practical applications in dermatology and comparison with established imaging methods. *Ski. Res. Technol.* **2021**, *27*, 340–352. [CrossRef] [PubMed]

104. Kirby, M.A.; Tang, P.; Liou, H.-C.; Kuriakose, M.; Pitre, J.J.; Pham, T.N.; Ettinger, R.E.; Wang, R.K.; O'Donnell, M.; Pelivanov, I. Probing elastic anisotropy of human skin in vivo with light using non-contact acoustic micro-tapping OCE and polarization sensitive OCT. *Sci. Rep.* **2022**, *12*, 3963. [CrossRef] [PubMed]

105. Makita, S.; Yasuno, Y. In vivo photothermal optical coherence tomography for non-invasive imaging of endogenous absorption agents. *Biomed. Opt. Express* **2015**, *6*, 1707–1725. [CrossRef] [PubMed]

106. Liu, H.; Mo, L.; Chen, H.; Chen, C.; Wu, J.; Tang, Z.; Guo, Z.; Hu, C.; Liu, Z. Carbon Dots with Intrinsic Bioactivities for Photothermal Optical Coherence Tomography, Tumor-Specific Therapy and Postoperative Wound Management. *Adv. Healthc. Mater.* **2022**, *11*, 2101448. [CrossRef] [PubMed]

107. Schwartz, M.; Levine, A.; Markowitz, O. Optical coherence tomography in dermatology. *Cutis* **2017**, *100*, 163–166. [PubMed]

108. Welzel, J. Optical coherence tomography in dermatology: A review. *Ski. Res. Technol.* **2001**, *7*, 1–9. [CrossRef] [PubMed]

109. Gambichler, T.; Moussa, G.; Sand, M.; Sand, D.; Altmeyer, P.; Hoffmann, K. Applications of optical coherence tomography in dermatology. *J. Dermatol. Sci.* **2005**, *40*, 85–94. [CrossRef] [PubMed]

110. Olsen, J.; Holmes, J.; Jemec, G.B. Advances in optical coherence tomography in dermatology—A review. *J. Biomed. Opt.* **2018**, *23*, 040901. [CrossRef] [PubMed]

111. Hojjatoleslami, S.; Avanaki, M.; Podoleanu, A.G. Image quality improvement in optical coherence tomography using Lucy–Richardson deconvolution algorithm. *Appl. Opt.* **2013**, *52*, 5663–5670. [CrossRef]

112. Adabi, S.; Rashedi, E.; Clayton, A.; Mohebbi-Kalkhoran, H.; Chen, X.-w.; Conforto, S.; Avanaki, M.N. Learnable despeckling framework for optical coherence tomography images. *J. Biomed. Opt.* **2018**, *23*, 016013. [CrossRef] [PubMed]

113. Turani, Z.; Fatemizadeh, E.; Adabi, S.; Mehregan, D.; Daveluy, S.; Nasiriavanaki, M. *Noise Reduction in OCT Skin Images*; SPIE: Bellingham, WA, USA, 2017; Volume 10137.

114. O'leary, S.; Fotouhi, A.; Turk, D.; Sriranga, P.; Rajabi-Estarabadi, A.; Nouri, K.; Daveluy, S.; Mehregan, D.; Nasiriavanaki, M. OCT image atlas of healthy skin on sun-exposed areas. *Ski. Res. Technol.* **2018**, *24*, 570–586. [CrossRef] [PubMed]

115. Hojjatoleslami, A.; Avanaki, M.R. OCT skin image enhancement through attenuation compensation. *Appl. Opt.* **2012**, *51*, 4927–4935. [CrossRef]

116. Nasiri-Avanaki, M.-R.; Hojjatoleslami, S.; Paun, H.; Tuohy, S.; Meadway, A.; Dobre, G.; Podoleanu, A. Optical coherence tomography system optimization using simulated annealing algorithm. *Proc. Math. Methods Appl. Comput.* **2009**, *669*, 552–557.

117. Adabi, S.; Turani, Z.; Fatemizadeh, E.; Clayton, A.; Nasiriavanaki, M. Optical coherence tomography technology and quality improvement methods for optical coherence tomography images of skin: A short review. *Biomed. Eng. Comput. Biol.* **2017**, *8*, 1179597217713475. [CrossRef] [PubMed]

118. Adabi, S.; Fotouhi, A.; Xu, Q.; Daveluy, S.; Mehregan, D.; Podoleanu, A.; Nasiriavanaki, M. An overview of methods to mitigate artifacts in optical coherence tomography imaging of the skin. *Ski. Res. Technol.* **2018**, *24*, 265–273. [CrossRef] [PubMed]

119. Turani, Z.; Fatemizadeh, E.; Xu, Q.; Daveluy, S.; Mehregan, D.; Nasiriavanaki, M. Refractive index correction in optical coherence tomography images of multilayer tissues. *J. Biomed. Opt.* **2018**, *23*, 070501. [CrossRef] [PubMed]

120. Avanaki, M.R.; Hojjatoleslami, A. Skin layer detection of optical coherence tomography images. *Optik* **2013**, *124*, 5665–5668. [CrossRef]

121. Avanaki, M.R.; Cernat, R.; Tadrous, P.J.; Tatla, T.; Podoleanu, A.G.; Hojjatoleslami, S.A. Spatial compounding algorithm for speckle reduction of dynamic focus OCT images. *IEEE Photonics Technol. Lett.* **2013**, *25*, 1439–1442. [CrossRef]

122. Avanaki, M.R.; Laissue, P.P.; Eom, T.J.; Podoleanu, A.G.; Hojjatoleslami, A. Speckle reduction using an artificial neural network algorithm. *Appl. Opt.* **2013**, *52*, 5050–5057. [CrossRef] [PubMed]

123. May, J.; Lee, J.; Puyana, C.; Tsoukas, M.; Avanaki, K. 40638 Comprehensive Atlas of Healthy Skin Using Optical Coherence Tomography. *J. Am. Acad. Dermatol.* **2023**, *89*, AB140. [CrossRef]

124. Taghavikhalilbad, A.; Adabi, S.; Clayton, A.; Soltanizadeh, H.; Mehregan, D.; Avanaki, M.R. Semi-automated localization of dermal epidermal junction in optical coherence tomography images of skin. *Appl. Opt.* **2017**, *56*, 3116–3121. [CrossRef] [PubMed]

125. Avanaki, M.R.; Podoleanu, A.G.; Price, M.C.; Corr, S.A.; Hojjatoleslami, S. Two applications of solid phantoms in performance assessment of optical coherence tomography systems. *Appl. Opt.* **2013**, *52*, 7054–7061. [CrossRef] [PubMed]

126. Herman, C. Emerging technologies for the detection of melanoma: Achieving better outcomes. *Clin. Cosmet. Investig. Dermatol.* **2012**, *5*, 195. [CrossRef] [PubMed]

127. Manwar, R.; Li, X.; Mahmoodkalayeh, S.; Asano, E.; Zhu, D.; Avanaki, K. Deep learning protocol for improved photoacoustic brain imaging. *J. Biophotonics* **2020**, *13*, e202000212. [CrossRef] [PubMed]

128. Kratkiewicz, K.; Manwar, R.; Zhou, Y.; Mozaffarzadeh, M.; Avanaki, K. Technical considerations in the Verasonics research ultrasound platform for developing a photoacoustic imaging system. *Biomed. Opt. Express* **2021**, *12*, 1050–1084. [CrossRef] [PubMed]

129. Kratkiewicz, K.; Manwar, R.; Rajabi-Estarabadi, A.; Fakhoury, J.; Meiliute, J.; Daveluy, S.; Mehregan, D.; Avanaki, K.M. Photoacoustic/Ultrasound/Optical Coherence Tomography Evaluation of Melanoma Lesion and Healthy Skin in a Swine Model. *Sensors* **2019**, *19*, 2815. [CrossRef] [PubMed]

130. Hariri, A.; Fatima, A.; Mohammadian, N.; Bely, N.; Nasiriavanaki, M. Towards low cost photoacoustic microscopy system for evaluation of skin health. In Proceedings of the Imaging Spectrometry XXI, San Diego, CA, USA, 19 September 2016; p. 99760X.

131. Siegel, A.P.; Avanaki, K. The power of light and sound: Optoacoustic skin imaging for diabetes progression monitoring. *Light: Sci. Appl.* **2023**, *12*, 283. [CrossRef] [PubMed]

132. Sinnamon, A.J.; Neuwirth, M.G.; Song, Y.; Schultz, S.M.; Liu, S.; Xu, X.; Sehgal, C.M.; Karakousis, G.C. Multispectral photoacoustic imaging for the detection of subclinical melanoma. *J. Surg. Oncol.* **2019**, *119*, 1070–1076. [CrossRef] [PubMed]

133. Kim, C.; Cho, E.C.; Chen, J.; Song, K.H.; Au, L.; Favazza, C.; Zhang, Q.; Cobley, C.M.; Gao, F.; Xia, Y. In vivo molecular photoacoustic tomography of melanomas targeted by bioconjugated gold nanocages. *ACS Nano* **2010**, *4*, 4559–4564. [CrossRef] [PubMed]

134. Kim, J.; Kim, Y.H.; Park, B.; Seo, H.M.; Bang, C.H.; Park, G.S.; Park, Y.M.; Rhie, J.W.; Lee, J.H.; Kim, C. Multispectral ex vivo photoacoustic imaging of cutaneous melanoma for better selection of the excision margin. *Br. J. Dermatol.* **2018**, *179*, 780–782. [CrossRef] [PubMed]

135. Breathnach, A.; Concannon, E.; Dorairaj, J.J.; Shaharan, S.; McGrath, J.; Jose, J.; Kelly, J.L.; Leahy, M.J. Preoperative measurement of cutaneous melanoma and nevi thickness with photoacoustic imaging. *J. Med. Imaging* **2018**, *5*, 015004. [CrossRef] [PubMed]

136. Wang, C.; Guo, L.; Wang, G.; Ye, T.; Wang, B.; Xiao, J.; Liu, X.J.A.O. In-vivo imaging of melanoma with simultaneous dual-wavelength acoustic-resolution-based photoacoustic/ultrasound microscopy. *Appl. Opt.* **2021**, *60*, 3772–3778. [CrossRef] [PubMed]

137. Stoffels, I.; Morscher, S.; Helfrich, I.; Hillen, U.; Leyh, J.; Burton, N.C.; Sardella, T.C.; Claussen, J.; Poeppel, T.D.; Bachmann, H.S.; et al. Metastatic status of sentinel lymph nodes in melanoma determined noninvasively with multispectral optoacoustic imaging. *Sci. Transl. Med.* **2015**, *7*, 317ra199. [CrossRef] [PubMed]

138. Breathnach, A.; Concannon, L.; Aalto, L.; Dorairaj, J.; Subhash, H.M.; Kelly, J.; Leahy, M.J. Assessment of cutaneous melanoma and pigmented skin lesions with photoacoustic imaging. In Proceedings of the Photonic Therapeutics and Diagnostics XI, San Francisco, CA, USA, 2–7 February 2013; pp. 19–23.

139. Oh, J.-T.; Li, M.-L.; Zhang, H.F.; Maslov, K.; Stoica, G.; Wang, L.V. Three-dimensional imaging of skin melanoma in vivo by dual-wavelength photoacoustic microscopy. *J. Biomed. Opt.* **2006**, *11*, 034032–034034. [CrossRef] [PubMed]

140. Park, B.; Bang, C.H.; Lee, C.; Han, J.H.; Choi, W.; Kim, J.; Park, G.S.; Rhie, J.W.; Lee, J.H.; Kim, C. 3D wide-field multispectral photoacoustic imaging of human melanomas in vivo: A pilot study. *J. Eur. Acad. Dermatol. Venereol.* **2021**, *35*, 669–676. [CrossRef] [PubMed]

141. Neuschmelting, V.; Lockau, H.; Ntziachristos, V.; Grimm, J.; Kircher, M.F. Lymph Node Micrometastases and In-Transit Metastases from Melanoma: In Vivo Detection with Multispectral Optoacoustic Imaging in a Mouse Model. *Radiology* **2016**, *280*, 137–150. [CrossRef]

142. He, H.; Schönmann, C.; Schwarz, M.; Hindelang, B.; Berezhnoi, A.; Steimle-Grauer, S.A.; Darsow, U.; Aguirre, J.; Ntziachristos, V. Fast raster-scan optoacoustic mesoscopy enables assessment of human melanoma microvasculature in vivo. *Nat. Commun.* **2022**, *13*, 2803. [CrossRef] [PubMed]

143. Visscher, M.O.; Burkes, S.A.; Randall Wickett, R.; Eaton, K.P. Chapter 38—From Image to Information: Image Processing in Dermatology and Cutaneous Biology. In *Imaging in Dermatology*; Hamblin, M.R., Avci, P., Gupta, G.K., Eds.; Academic Press: Boston, MA, USA, 2016; pp. 519–535. [CrossRef]

144. Lao, Y.; Xing, D.; Yang, S. *Noninvasive Mapping of Subcutaneous Vasculature with High Resolution Photoacoustic Imaging*; SPIE: Bellingham, WA, USA, 2008; Volume 6826.

145. He, H.; Fasoula, N.-A.; Karlas, A.; Omar, M.; Aguirre, J.; Lutz, J.; Kallmayer, M.; Füchtenbusch, M.; Eckstein, H.-H.; Ziegler, A. Opening a window to skin biomarkers for diabetes stage with optoacoustic mesoscopy. *Light Sci. Appl.* **2023**, *12*, 231. [CrossRef] [PubMed]

146. Weber, J.; Beard, P.C.; Bohndiek, S.E. Contrast agents for molecular photoacoustic imaging. *Nat. Methods* **2016**, *13*, 639. [CrossRef] [PubMed]

147. Wu, D.; Huang, L.; Jiang, M.S.; Jiang, H. Contrast Agents for Photoacoustic and Thermoacoustic Imaging: A Review. *Int. J. Mol. Sci.* **2014**, *15*, 23616–23639. [CrossRef] [PubMed]

148. Attia, A.B.E.; Balasundaram, G.; Moothanchery, M.; Dinish, U.; Bi, R.; Ntziachristos, V.; Olivo, M. A review of clinical photoacoustic imaging: Current and future trends. *Photoacoustics* **2019**, *16*, 100144. [CrossRef] [PubMed]

149. Han, S.; Lee, D.; Kim, S.; Kim, H.H.; Jeong, S.; Kim, J. Contrast Agents for Photoacoustic Imaging: A Review Focusing on the Wavelength Range. *Biosensors* **2022**, *12*, 594. [CrossRef]

150. Lutzweiler, C.; Meier, R.; Rummeny, E.; Ntziachristos, V.; Razansky, D. Real-time optoacoustic tomography of indocyanine green perfusion and oxygenation parameters in human finger vasculature. *Opt. Lett.* **2014**, *39*, 4061–4064. [CrossRef] [PubMed]

151. Zeitouni, N.C.; Rohrbach, D.J.; Aksahin, M.; Sunar, U. Preoperative Ultrasound and Photoacoustic Imaging of Nonmelanoma Skin Cancers. *Dermatol. Surg.* **2015**, *41*, 525–528. [CrossRef] [PubMed]

152. Zhou, Y.; Huang, X.; Li, J.; Zhu, T.; Pang, W.; Chow, L.; Nie, L.; Sun, L.; Lai, P. Small Animal In Situ Drug Delivery Effects via Transdermal Microneedles Array versus Intravenous Injection: A Pilot Observation Based on Photoacoustic Tomography. *Pharmaceutics* **2022**, *14*, 2689. [CrossRef] [PubMed]

153. Park, B.; Park, S.; Kim, J.; Kim, C. Listening to drug delivery and responses via photoacoustic imaging. *Adv. Drug Deliv. Rev.* **2022**, *184*, 114235. [CrossRef] [PubMed]

154. Sivasubramanian, K.; Mathiyazhakan, M.; Wiraja, C.; Upputuri, P.K.; Xu, C.; Pramanik, M. Near-infrared light-responsive liposomal contrast agent for photoacoustic imaging and drug release applications. *J. Biomed. Opt.* **2017**, *22*, 041007. [CrossRef] [PubMed]

155. Hariri, A.; Chen, F.; Moore, C.; Jokerst, J.V. Noninvasive staging of pressure ulcers using photoacoustic imaging. *Wound Repair Regen.* **2019**, *27*, 488–496. [CrossRef]

156. Ida, T.; Iwazaki, H.; Kawaguchi, Y.; Kawauchi, S.; Ohkura, T.; Iwaya, K.; Tsuda, H.; Saitoh, D.; Sato, S.; Iwai, T. Burn depth assessments by photoacoustic imaging and laser Doppler imaging. *Wound Repair Regen.* **2016**, *24*, 349–355. [CrossRef] [PubMed]

157. Ida, T.; Kawaguchi, Y.; Kawauchi, S.; Iwaya, K.; Tsuda, H.; Saitoh, D.; Sato, S.; Iwai, T. Real-time photoacoustic imaging system for burn diagnosis. *J. Biomed. Opt.* **2014**, *19*, 086013. [CrossRef]

158. Nam, S.Y.; Chung, E.; Suggs, L.J.; Emelianov, S.Y. Combined Ultrasound and Photoacoustic Imaging to Noninvasively Assess Burn Injury and Selectively Monitor a Regenerative Tissue-Engineered Construct. *Tissue Eng. Part C Methods* **2015**, *21*, 557–566. [CrossRef] [PubMed]

159. Mantri, Y.; Tsujimoto, J.; Donovan, B.; Fernandes, C.C.; Garimella, P.S.; Penny, W.F.; Anderson, C.A.; Jokerst, J.V. Photoacoustic monitoring of angiogenesis predicts response to therapy in healing wounds. *Wound Repair Regen.* **2022**, *30*, 258–267. [CrossRef]

160. Wang, Y.; Zhan, Y.; Harris, L.M.; Khan, S.; Xia, J. A portable three-dimensional photoacoustic tomography system for imaging of chronic foot ulcers. *Quant. Imaging Med. Surg.* **2019**, *9*, 799. [CrossRef] [PubMed]

161. Hariri, A.; Moore, C.; Mantri, Y.; Jokerst, J.V. Photoacoustic Imaging as a Tool for Assessing Hair Follicular Organization. *Sensors* **2020**, *20*, 5848. [CrossRef] [PubMed]

162. Zhang, D.; Yuan, Y.; Zhang, H.; Yi, X.; Xiao, W.; Yu, A. Photoacoustic Microscopy Provides Early Prediction of Tissue Necrosis in Skin Avulsion Injuries. *Clin. Cosmet. Investig. Dermatol.* **2021**, *14*, 837–844. [CrossRef] [PubMed]

163. Wang, Z.; Yang, F.; Zhang, W.; Yang, S. Quantitative and anatomical imaging of human skin by noninvasive photoacoustic dermoscopy. *Bio-Protoc.* **2022**, *12*, e4372. [CrossRef] [PubMed]

164. Hindelang, B.; Aguirre, J.; Schwarz, M.; Berezhnoi, A.; Eyerich, K.; Ntziachristos, V.; Biedermann, T.; Darsow, U. Non-invasive imaging in dermatology and the unique potential of raster-scan optoacoustic mesoscopy. *J. Eur. Acad. Dermatol. Venereol.* **2019**, *33*, 1051–1061. [CrossRef]

165. Aguirre, J.; Schwarz, M.; Garzorz, N.; Omar, M.; Buehler, A.; Eyerich, K.; Ntziachristos, V. Precision assessment of label-free psoriasis biomarkers with ultra-broadband optoacoustic mesoscopy. *Nat. Biomed. Eng.* **2017**, *1*, 0068. [CrossRef]

166. Geisler, E.L.; Brannen, A.; Pressler, M.; Perez, J.; Kane, A.A.; Hallac, R.R. 3D imaging of vascular anomalies using raster-scanning optoacoustic mesoscopy. *Lasers Surg. Med.* **2022**, *54*, 1269–1277. [CrossRef]

167. He, H.; Paetzold, J.C.; Börner, N.; Riedel, E.; Gerl, S.; Schneider, S.; Fisher, C.; Ezhov, I.; Shit, S.; Li, H. Machine learning analysis of human skin by optoacoustic mesoscopy for automated extraction of psoriasis and aging biomarkers. *IEEE Trans. Med. Imaging* **2024**. [CrossRef]

168. Nitkunanantharajah, S.; Haedicke, K.; Moore, T.B.; Manning, J.B.; Dinsdale, G.; Berks, M.; Taylor, C.; Dickinson, M.R.; Jüstel, D.; Ntziachristos, V.; et al. Three-dimensional optoacoustic imaging of nailfold capillaries in systemic sclerosis and its potential for disease differentiation using deep learning. *Sci. Rep.* **2020**, *10*, 16444. [CrossRef] [PubMed]

169. Wu, Z.; Duan, F.; Zhang, J.; Li, S.; Ma, H.; Nie, L. In vivo dual-scale photoacoustic surveillance and assessment of burn healing. *Biomed. Opt. Express* **2019**, *10*, 3425–3433. [CrossRef] [PubMed]

170. Roberts, W.E. Skin type classification systems old and new. *Dermatol. Clin.* **2009**, *27*, 529–533. [CrossRef]

171. Deán-Ben, X.L.; Razansky, D. Optoacoustic imaging of the skin. *Exp. Dermatol.* **2021**, *30*, 1598–1609. [CrossRef] [PubMed]

172. Kukk, A.F.; Scheling, F.; Panzer, R.; Emmert, S.; Roth, B. Combined ultrasound and photoacoustic C-mode imaging system for skin lesion assessment. *Sci. Rep.* **2023**, *13*, 17947. [CrossRef] [PubMed]

173. Daoudi, K.; Kersten, B.E.; van den Ende, C.H.; van den Hoogen, F.H.; Vonk, M.C.; de Korte, C.L. Photoacoustic and high-frequency ultrasound imaging of systemic sclerosis patients. *Arthritis Res. Ther.* **2021**, *23*, 22. [CrossRef] [PubMed]

174. Wen, Y.; Huang, Y.; Huang, L.; Wu, D.; Zhong, R.; Jiang, S.; Zhang, Y.; Liu, T.; Liu, X.; Jiang, H. Photoacoustic/Ultrasound Dual-Modal Imaging of Human Nails: A pilot study. *J. Innov. Opt. Health Sci.* **2004**, *18*, 010502. [CrossRef]

175. Seeger, M.; Dehner, C.; Jüstel, D.; Ntziachristos, V. Label-free concurrent 5-modal microscopy (Co5M) resolves unknown spatio-temporal processes in wound healing. *Commun. Biol.* **2021**, *4*, 1040. [CrossRef] [PubMed]

176. Liu, N.; Chen, Z.; Xing, D. Integrated photoacoustic and hyperspectral dual-modality microscopy for co-imaging of melanoma and cutaneous squamous cell carcinoma in vivo. *J. Biophotonics* **2020**, *13*, e202000105. [CrossRef] [PubMed]

177. Dontu, S.; Miclos, S.; Savastru, D.; Tautan, M. Combined spectral-domain optical coherence tomography and hyperspectral imaging applied for tissue analysis: Preliminary results. *Appl. Surf. Sci.* **2017**, *417*, 119–123. [CrossRef]

178. Chen, Z.; Rank, E.; Meiburger, K.M.; Sinz, C.; Hodul, A.; Zhang, E.; Hoover, E.; Minneman, M.; Ensher, J.; Beard, P.C. Non-invasive multimodal optical coherence and photoacoustic tomography for human skin imaging. *Sci. Rep.* **2017**, *7*, 17975. [CrossRef] [PubMed]

179. Zhang, E.Z.; Povazay, B.; Laufer, J.; Alex, A.; Hofer, B.; Pedley, B.; Glittenberg, C.; Treeby, B.; Cox, B.; Beard, P. Multimodal photoacoustic and optical coherence tomography scanner using an all optical detection scheme for 3D morphological skin imaging. *Biomed. Opt. Express* **2011**, *2*, 2202–2215. [CrossRef] [PubMed]

180. Kukk, A.F.; Wu, D.; Gaffal, E.; Panzer, R.; Emmert, S.; Roth, B. Multimodal imaging system with ultrasound, photoacoustics, and optical coherence tomography for optical biopsy of melanoma. In Proceedings of the Multimodal Biomedical Imaging XVIII, San Francisco, CA, USA, 28 January 2023; pp. 16–22.

181. Varkentin, A.; Mazurenka, M.; Blumenröther, E.; Behrendt, L.; Emmert, S.; Morgner, U.; Meinhardt-Wollweber, M.; Rahlves, M.; Roth, B. Trimodal system for in vivo skin cancer screening with combined optical coherence tomography-Raman and colocalized optoacoustic measurements. *J. Biophotonics* **2018**, *11*, e201700288. [CrossRef] [PubMed]

182. Liu, K.; Chen, Z.; Zhou, W.; Xing, D. Towards quantitative assessment of burn based on photoacoustic and optical coherence tomography. *J. Biophotonics* **2020**, *13*, e202000126. [CrossRef] [PubMed]

183. Gambichler, T.; Pljakic, A.; Schmitz, L. Recent advances in clinical application of optical coherence tomography of human skin. *Clin. Cosmet. Investig. Dermatol.* **2015**, *8*, 345–354. [CrossRef] [PubMed]

184. Spaide, R.F.; Otto, T.; Caujolle, S.; Kübler, J.; Aumann, S.; Fischer, J.; Reisman, C.; Spahr, H.; Lessmann, A. Lateral resolution of a commercial optical coherence tomography instrument. *Transl. Vis. Sci. Technol.* **2022**, *11*, 28. [CrossRef] [PubMed]

185. Felice, S.; Bressler, M.Y.; Karim, R.; Markowitz, O. Transforming the treatment of psoriasis to the 21st century: Detecting subclinical therapeutic response to secukinumab using optical coherence tomography as a prognostic indicator. *Lasers Surg. Med.* **2022**, *54*, 825–834. [CrossRef] [PubMed]

186. Hindelang, B.; Nau, T.; Englert, L.; Berezhnoi, A.; Lauffer, F.; Darsow, U.; Biedermann, T.; Eyerich, K.; Aguirre, J.; Ntziachristos, V. Enabling precision monitoring of psoriasis treatment by optoacoustic mesoscopy. *Sci. Transl. Med.* **2022**, *14*, eabm8059. [CrossRef] [PubMed]

187. Duan, M.; Byers, R.A.; Danby, S.G.; Sahib, S.; Cha, A.; Zang, C.; Werth, J.; Adiri, R.; Taylor, R.N.; Cork, M.J. Potential application of PS-OCT in the safety assessment of non-steroidal topical creams for atopic dermatitis treatment. *Biomed. Opt. Express* **2023**, *14*, 4126–4136. [CrossRef] [PubMed]

188. Yew, Y.W.; Amma, D.U.K.S.; Kuan, A.H.Y.; Li, X.; Dev, K.; Attia, A.B.E.; Bi, R.; Moothanchery, M.; Balasundaram, G.; Aguirre, J. Raster-scanning optoacoustic mesoscopy imaging as an objective disease severity tool in atopic dermatitis patients. *J. Am. Acad. Dermatol.* **2021**, *84*, 1121–1123. [CrossRef] [PubMed]

189. Moothanchery, M.; Attia, A.B.E.; Xiuting, L.; Weng, Y.Y.; Guan, S.T.T.; Dinish, U.; Olivo, M. Assessment of oxygen saturation in microvasculature of atopic dermatitis patients using multispectral optoacoustic mesoscopy. In Proceedings of the Photonic Diagnosis, Monitoring, Prevention, and Treatment of Infections and Inflammatory Diseases 2022, San Francisco, CA, USA, 3–4 February 2020; p. 1193902.

190. Attia, A.B.E.; Chuah, S.Y.; Razansky, D.; Ho, C.J.H.; Malempati, P.; Dinish, U.; Bi, R.; Fu, C.Y.; Ford, S.J.; Lee, J.S.-S.J.P. Noninvasive real-time characterization of non-melanoma skin cancers with handheld optoacoustic probes. *Photoacoustics* **2017**, *7*, 20–26. [CrossRef] [PubMed]

191. Hult, J.; Dahlstrand, U.; Merdasa, A.; Wickerström, K.; Chakari, R.; Persson, B.; Cinthio, M.; Erlöv, T.; Albinsson, J.; Gesslein, B. Unique spectral signature of human cutaneous squamous cell carcinoma by photoacoustic imaging. *J. Biophotonics* **2020**, *13*, e201960212. [CrossRef] [PubMed]

192. Marjanovic, E.; Sharma, V.; Smith, L.; Pinder, C.; Moore, T.; Manning, J.; Dinsdale, G.; Berks, M.; Newton, V.; Wilkinson, S. Polarisation-sensitive optical coherence tomography measurement of retardance in fibrosis, a non-invasive biomarker in patients with systemic sclerosis. *Sci. Rep.* **2022**, *12*, 2893. [CrossRef] [PubMed]

193. Abignano, G.; Karadağ, D.T.; Gundogdu, O.; Lettieri, G.; Padula, M.; Padula, A.; Emery, P.; D'angelo, S.; Del Galdo, F. *FRI0226 Optical Coherence Tomography of the Skin Detects Scleroderma Changes in Clinically Unaffected Skin: An Opportunity for Early Detection of Systemic Sclerosis*; BMJ Publishing Group Ltd.: Hoboken, NJ, USA, 2020.

194. Lee, J.; Beirami, M.J.; Ebrahimpour, R.; Puyana, C.; Tsoukas, M.; Avanaki, K. Optical coherence tomography confirms non-malignant pigmented lesions in phacomatosis pigmentokeratotica using a support vector machine learning algorithm. *Ski. Res. Technol.* **2023**, *29*, e13377. [CrossRef] [PubMed]

195. Ghosh, B.; Mandal, M.; Mitra, P.; Chatterjee, J. Attenuation corrected-optical coherence tomography for quantitative assessment of skin wound healing and scar morphology. *J. Biophotonics* **2021**, *14*, e202000357. [CrossRef] [PubMed]

196. Deegan, A.J.; Mandell, S.P.; Wang, R.K. Optical coherence tomography correlates multiple measures of tissue damage following acute burn injury. *Quant. Imaging Med. Surg.* **2019**, *9*, 731. [CrossRef] [PubMed]

197. Moore, C.; Jokerst, J.V. Strategies for Image-Guided Therapy, Surgery, and Drug Delivery Using Photoacoustic Imaging. *Theranostics* **2019**, *9*, 1550–1571. [CrossRef] [PubMed]